

# Aminated Quinolinequinones as Privileged Scaffolds for Antibacterial Agents: Synthesis, *In Vitro* Evaluation, and Putative Mode of Action

Hatice Yıldırım, Nilüfer Bayrak, Mahmut Yıldız, Emel Mataracı-Kara, Serol Korkmaz, Deepak Shilkar, Venkatesan Jayaprakash, and Amaç Fatih TuYuN\*



Cite This: *ACS Omega* 2022, 7, 41915–41928



Read Online

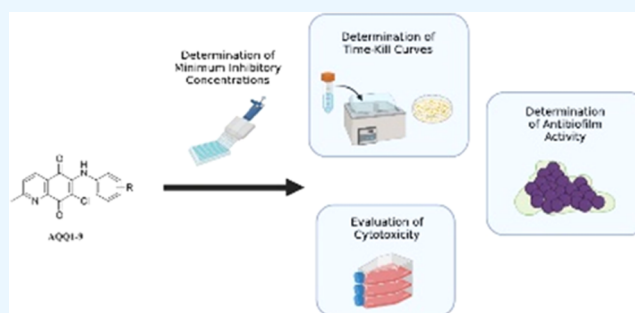
ACCESS |

Metrics & More

Article Recommendations

Supporting Information

**ABSTRACT:** Our previous studies have revealed that the aminated 1,4-quinone scaffold can be used for the development of novel antibacterial and/or antifungal agents. In this study, the aminated quinolinequinones (AQQ1–9) were designed, synthesized, and evaluated for their antimicrobial activity against a panel of seven bacterial strains (three Gram-positive and four Gram-negative bacteria) and three fungal strains. The structure–activity relationship (SAR) for the QQs was also summarized. The antibacterial activity results indicated that the two aminated QQs (AQQ6 and AQQ9) were active against *Enterococcus faecalis* (ATCC 29212) with a MIC value of 78.12  $\mu\text{g}/\text{mL}$ . Besides, the two aminated QQs (AQQ8 and AQQ9) were active against *Staphylococcus aureus* (ATCC 29213) with MIC values of 4.88 and 2.44  $\mu\text{g}/\text{mL}$ , respectively. The most potent aminated QQs (AQQ8 and AQQ9) were identified as promising lead molecules to further explore their mode of action. The selected QQs (AQQ8 and AQQ9) were further evaluated *in vitro* to assess their potential antimicrobial activity against each of 20 clinically obtained methicillin-resistant *S. aureus* isolates, antibiofilm activity, and bactericidal activity using time-kill curve assay. We found that the molecules prevented adhesion of over 50% of the cells in the biofilm. Molecular docking studies were performed to predict the predominant binding mode(s) of the ligands. We believe that the molecules need further investigation, especially against infections involving biofilm-forming microbes.



## 1. INTRODUCTION

Antimicrobial resistance (AMR) has raised even more serious concerns with the advent of the COVID-19 pandemic. Studies have shown that alongside SARS-CoV-2 infection, increased antimicrobial resistance has dealt another heavy blow to COVID-19 patients. Notably, the heavy antibiotic use during the pandemic has given rise to multidrug-resistant organisms (MDROs).<sup>1</sup> The emergence of MDROs can be prevented by judicious prescription, optimal drug use, and aggressive infection control.<sup>2</sup> The relationship between the use of antibiotics and the development of AMR has been well studied.<sup>3</sup> The AMR threat has increasingly emerged worldwide for every antibacterial and/or antifungal drug on the market. Mainly, methicillin-resistant *Staphylococcus aureus* (MRSA) has emerged as one of the most dangerous pathogenic bacteria<sup>4</sup> causing fatal infections such as sepsis, meningitis, pneumonia, or skin infections. It has also developed resistance against several antibiotics, such as vancomycin, which has been dubbed the “antibiotic of last resort”. The first documented case of resistance against vancomycin was reported in 2002.<sup>5</sup> Thereafter, daptomycin was approved by the United States Food and Drug Administration (FDA) in 2003 as the last new

drug class.<sup>6</sup> The time from the release of a drug to the emergence of resistance is approximately 10 years,<sup>7</sup> and shorter duration has been observed in diseases like tuberculosis. Therefore, there is a great deal of urgency to release antimicrobial drugs with broad- and/or specific-spectrum biological properties into the market to fight clinical resistance.

Considering that 1,4-quinone moiety is reportedly active against several types of pathogens, including Gram-positive and Gram-negative bacteria, fungi, as well as viruses, researchers have continued to explore 1,4-quinone core as potential antibacterial,<sup>8</sup> antifungal,<sup>9</sup> and antiviral agents<sup>10</sup> to understand their mode of actions. Some important drugs, such as mitomycin C, mitoxantrone, and doxorubicin containing 1,4-quinone moiety in their structures, have been approved for

Received: May 22, 2022

Accepted: October 25, 2022

Published: November 9, 2022



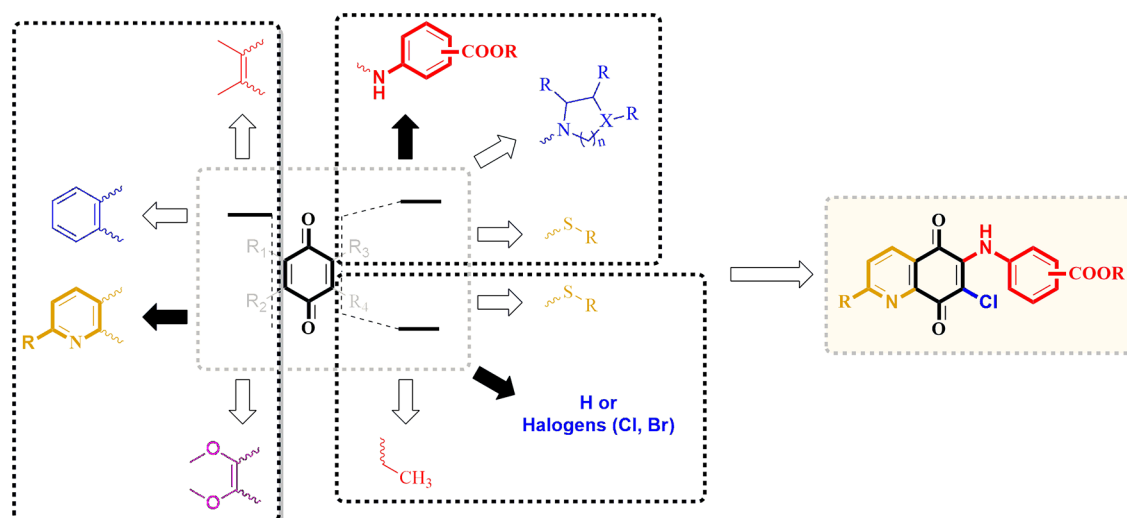


**Figure 1.** Design strategy by the incorporation of quinolinequinone and aryl amines containing ester group in different positions as the substrates based on our previous results in the literature.

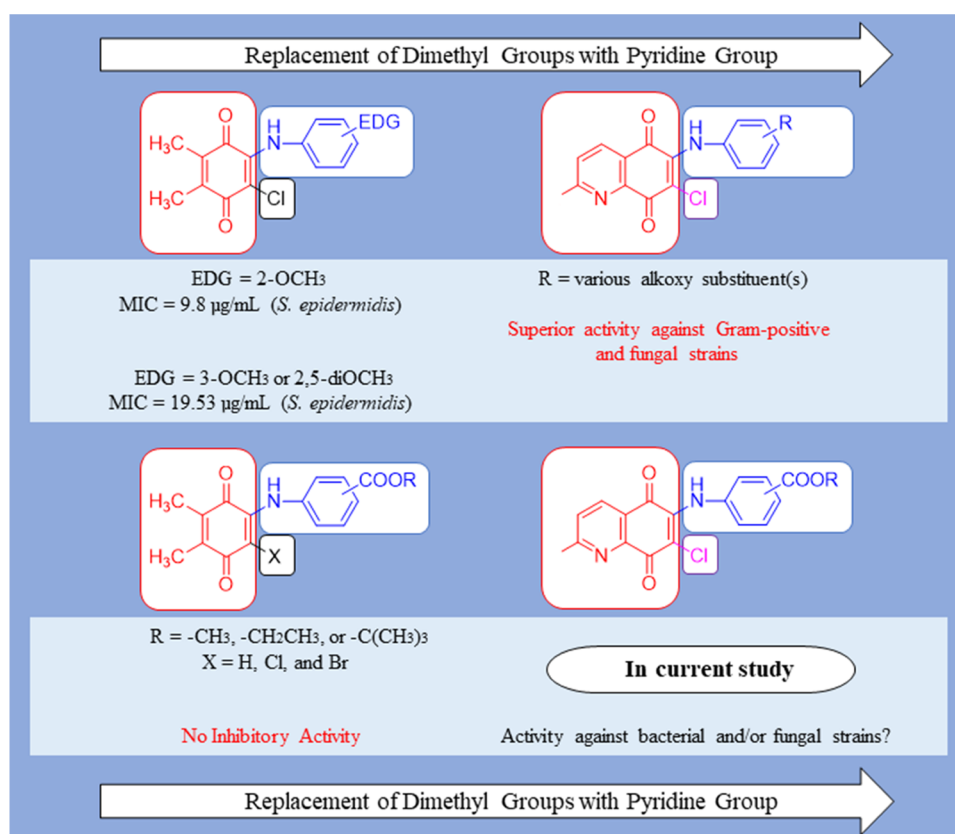


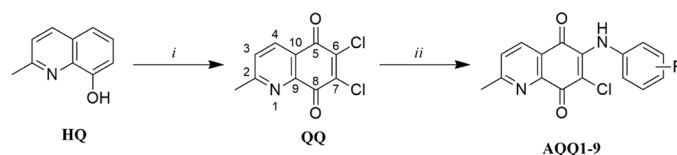
**Figure 2.** Design strategy by the incorporation of both quinone moiety and aryl amines containing an ester group.

clinical use by the U.S. Food and Drug Administration (FDA).<sup>11</sup> Additionally, a large and growing body of literature has highlighted that 1,4-quinone moiety serves as the main skeleton for several natural and synthetic pharmacologically active compounds.<sup>12</sup> Moreover, the amine functional group inserted into the 1,4-quinone moiety represented one of the most significant core structures incorporated into organic and medicinal chemistry.

The development of new drug candidates involves several different stages that are highly time-consuming and expensive, with a high risk of failure starting from target identification,

lead identification and optimization, preclinical and toxicity studies, formulation, clinical trial, approval, and marketing. In the past 10 years or so, we have been developing potential drug candidates in our laboratory to fight cancer and antimicrobial resistance and have primarily modified a 1,4-quinone moiety with different side groups to find out the structure–activity relationships (SARs) around this moiety as shown in Figure 1.<sup>13–15</sup> The insertion of primary or secondary amines and/or aromatic/alkyl chain thiols into the 1,4-quinone moiety is our primary goal. Besides, we have also tuned the biological activity of quinones through the modification of this moiety, fused with

## Scheme 1. Regioselective Preparation of the Aminated QQs (AQQ1–9)



(i)  $\text{NaClO}_3$ , HCl, 50–60°C; (ii)  $\text{CeCl}_3 \cdot 7\text{H}_2\text{O}$ , corresponding aryl anilines, EtOH, rt to reflux, 3–6 h. Arbitrary numbering is for NMR assignments.

ID	R	ID	R	ID	R
AQQ1	2-COOCH <sub>3</sub>	AQQ4	2-COOCH <sub>2</sub> CH <sub>3</sub>	AQQ7	2-COOC(CH <sub>3</sub> ) <sub>3</sub>
AQQ2	3-COOCH <sub>3</sub>	AQQ5	3-COOCH <sub>2</sub> CH <sub>3</sub>	AQQ8	3-COOC(CH <sub>3</sub> ) <sub>3</sub>
AQQ3	4-COOCH <sub>3</sub>	AQQ6	4-COOCH <sub>2</sub> CH <sub>3</sub>	AQQ9	4-COOC(CH <sub>3</sub> ) <sub>3</sub>

benzene named as naphthoquinone analogues (vitamin K analogues),<sup>16</sup> or fused with pyridine named as quinolinequinone analogues,<sup>13,17,18</sup> or attached to the dimethoxy groups named as Coenzyme Q analogues,<sup>19</sup> or attached to the dimethyl groups named as Plastoquinone analogues.<sup>14,20</sup> Our initial structure–activity relationship (SAR) studies focused on exploring the effect of 1,4-quinone moiety, in addition to the type of amino moiety, the substituent(s) within amino moiety, and the type of halogen (bromine or chlorine atom) as the side chains. The antimicrobial activity and structures of these molecules are shown in Figure 2. We found that aryl amines containing electron-donating group (EDG) attached to the chlorinated dimethylbenzoquinone positively influence antibacterial activity, while chlorinated dimethylbenzoquinones containing aryl amine, substituted with electron-withdrawing group (EWG), do not show any inhibition efficacy.<sup>15</sup> Recently, we have designed a series of nonhalogenated and halogenated (brominated and chlorinated) aminobenzoquinones, which integrated the merits of both a dimethylquinone moiety and aryl amines containing an ester group in different positions.<sup>21</sup> These molecules did not have any Gram-positive and Gram-negative antibacterial activity, in addition to antifungal activity. Last but not least, the modification of 1,4-quinone moiety by replacing dimethyl groups with a pyridine moiety, named quinolinequinones (QQs), yielded promising results.

In this study, we report the design, synthesis, antimicrobial evaluation, and SAR analysis of a series of chlorinated QQs with aryl amines containing ester group in different positions to investigate the effect of such structural modifications on the biological activity profile.<sup>13,17</sup> Owing to the importance of all of the available information, the most remarkable members of the chlorinated QQs with aryl amines containing ester group were tested for their antibiofilm activity and potential antimicrobial activity against each of 20 clinically obtained strains of methicillin-resistant *S. aureus*, and bactericidal time-kill kinetic study. We also performed *in silico* evaluation to assess and possibly estimate the mechanism of action of these compounds. Thioredoxin reductase 1 is a homodimeric flavoprotein critical for redox regulation of protein function and is involved in regulating cellular redox reactions that are crucial for the survival of various bacterial species by helping them combat oxidative stress.<sup>22</sup> Studies have shown its importance in the survival of *S. aureus*, and others have also targeted the thioredoxin system.<sup>23</sup> Polynucleotide phosphorylase (PNPase) is a bifunctional exoribonuclease responsible for mRNA turnover by dismantling the RNA chain starting at the 3' end and working toward the 5' end and synthesizing long, highly heteropolymeric tails *in vivo*.<sup>24</sup> It acts as quality

control for rRNA precursors in several bacteria, including *S. aureus*. We retrieved these proteins from the AlphaFold database for *S. aureus* (strain MRSA252) to perform molecular docking studies for our compounds since they have been reported to play a significant role in the survival of our target microorganisms.

## 2. RESULTS AND DISCUSSION

**2.1. Chemistry.** The synthesis of the aminated QQs (AQQ1–9) began with the conversion of the commercially available hydroxyquinoline (HQ) to the dichloroquinolinequinone (QQ) in one step with sodium chlorate in concentrated HCl solution<sup>25</sup> with a slight modification as shown in Scheme 1. According to the reported literature, the aminated QQs (AQQ1–9) were regioselectively then formed upon treatment with corresponding aryl amines containing an ester group in the presence of the catalyst  $\text{CeCl}_3 \cdot 7\text{H}_2\text{O}$ .<sup>26</sup> Studies in the literature have revealed that regioselective nucleophilic substitution of dichloroquinolinequinone (QQ) at the C6 and/or C7 positions could give two different isomers since it contains two asymmetric chlorine atoms at the C6 and C7 positions.<sup>27</sup> The solvent used in the reaction medium plays a vital role in the reactions, i.e., protic solvents such as ethanol or water promote the substitution with the chlorine atom at the C6 position.<sup>27,28</sup>

To synthesize the aminated QQs, AQQ1–9 were regioselectively obtained by the amination reaction of 6,7-dichloro-2-methyl-5,8-quinolinequinone (QQ) in the presence of  $\text{CeCl}_3 \cdot 7\text{H}_2\text{O}$  with the corresponding aryl amines containing ester at *o*-, *m*-, and *p*- positions in ethanol. The aminated QQs (AQQ1–9) were purified via silica gel column chromatography. The structures of the aminated QQs were elucidated by Fourier transform infrared (FTIR) spectroscopy, <sup>1</sup>H nuclear magnetic resonance (NMR), <sup>13</sup>C NMR, and high-resolution mass spectrometry (HRMS). Additionally, X-ray crystallographic studies have also confirmed the regioselective amination of QQs at the C6 position in accordance with the literature.<sup>26,29</sup>

In addition to QQ, the molecular structure of AQQ2 was characterized using the single-crystal X-ray crystallographic analysis. These QQs (QQ and AQQ2) were dissolved in ethanol and kept for crystallization to yield high-quality diffraction crystals for at least 1 week. To confirm the regioselectivity of the substitution reactions, X-ray diffraction analyses were performed for the compound AQQ2. It has been found that the compound AQQ2 contains the aromatic amino group at the C6 position. Moreover, the X-ray diffraction analysis confirmed that AQQ2 is a 6-substituted isomer. Figure

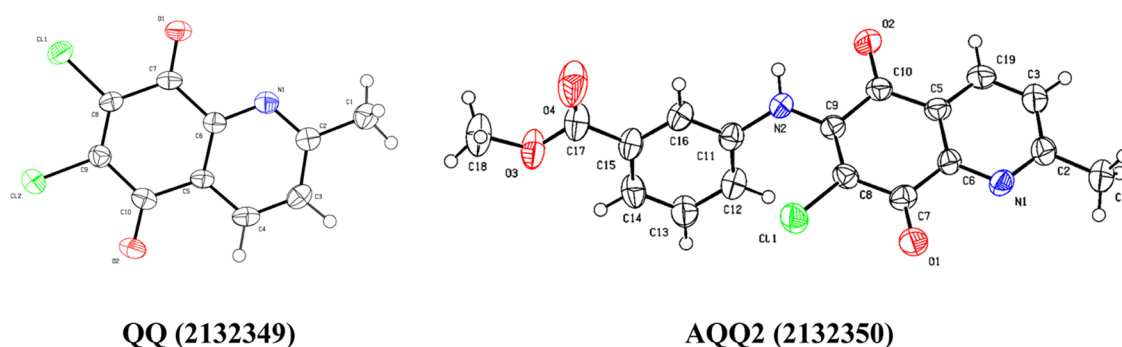


Figure 3. ORTEP drawings of QQ and AQQ2 at a 50% probability level.

Table 1. Crystallographic Data for the QQ and AQQ2

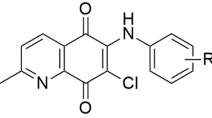
identification code	QQ	AQQ2
chemical formula	C <sub>10</sub> H <sub>5</sub> Cl <sub>2</sub> NO <sub>2</sub>	C <sub>18</sub> H <sub>13</sub> ClN <sub>2</sub> O <sub>4</sub>
formula weight (g mol <sup>-1</sup> )	242.05	356.75
temperature (K)	173(2)	273(2)
radiation λ (Å)	0.71073	0.71073
crystal system	monoclinic	orthorhombic
space groups, Z	P121/c1, 4	C222 <sub>1</sub> , 8
unit cell dimensions (Å)	<i>a</i> = 8.8264(6) <i>b</i> = 13.1484(8) <i>c</i> = 8.3983(5) <i>α</i> , <i>γ</i> = 90° <i>β</i> = 99.387(4)°	<i>a</i> = 8.1589(9) <i>b</i> = 15.1520(18) <i>c</i> = 25.806(3) <i>α</i> , <i>β</i> , <i>γ</i> = 90°
volume (Å <sup>3</sup> )	961.60(11)	3190.2(6)
crystal sizes (mm)	0.142 × 0.158 × 0.254	0.058 × 0.207 × 0.218
<i>d</i> <sub>calc</sub> (g cm <sup>-3</sup> )	1.672	1.486
absorption coefficient (mm <sup>-1</sup> )	0.648	0.266
absorption correction, <i>T</i> <sub>min</sub> , <i>T</i> <sub>max</sub>	multiscan, 0.8530, 0.9140	0.9440, 0.9850
<i>θ</i> <sub>max</sub> deg	25.0	25.07
goodness-of-fit on <i>F</i> <sup>2</sup>	1.036	1.081
index ranges	-10 ≤ <i>h</i> ≤ 10 -15 ≤ <i>k</i> ≤ 10 -7 ≤ <i>l</i> ≤ 9	-9 ≤ <i>h</i> ≤ 9 -17 ≤ <i>k</i> ≤ 18 -30 ≤ <i>l</i> ≤ 30
reflections collected	5014	18 234
independent reflections	1684 [ <i>R</i> (int) = 0.0554]	2846 [ <i>R</i> <sub>int</sub> = 0.0573]
final <i>R</i> indices [ <i>I</i> > 2σ( <i>I</i> )]	1178 data <i>R</i> <sub>1</sub> = 0.0446 <i>wR</i> <sub>2</sub> = 0.0983	2166 data <i>R</i> <sub>1</sub> = 0.0489 <i>wR</i> <sub>2</sub> = 0.0922
<i>R</i> indices (all data)	<i>R</i> <sub>1</sub> = 0.0739 <i>wR</i> <sub>2</sub> = 0.1093	<i>R</i> <sub>1</sub> = 0.0746 <i>wR</i> <sub>2</sub> = 0.0995
refinement method	full-matrix least-squares on <i>F</i> <sup>2</sup>	full-matrix least-squares on <i>F</i> <sup>2</sup>
data/restraints/parameters	1684/0/138	2846/0/228
largest diff. peak and hole (e Å <sup>-3</sup> )	0.317 and -0.265	0.172 and -0.155

3 presents ORTEP drawings of the QQ and AQQ2 at a 50% probability level. The crystallographic and structure refinement data for QQ and AQQ2 are summarized in Table 1. The details of all crystallographic data of the QQ and AQQ2 are presented in Tables S1–S4 in the Supporting Information.

The QQ crystallized in the monoclinic crystal system (space group P121/c1) with the unit cell parameters *a* = 8.8264(6), *b* = 13.1484(8), *c* = 8.3983(5), *α*, *γ* = 90°, *β* = 99.387(4)°. The AQQ2 crystallized in the orthorhombic crystal system (space group C222<sub>1</sub>) with the unit cell parameters *a* = 8.1589(9), *b* = 15.1520(18), *c* = 25.806(3), *α*, *β*, *γ* = 90°. The unit cell of QQ contains four molecules, while the unit cell of the AQQ2 contains eight molecules (Table 1). The distances between the C and N atoms of the quinoline ring in the QQ and AQQ2

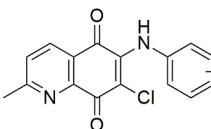
were approximately 1.34 Å. The lengths of the C=O bonds on the benzoquinone ring of both QQs were about 1.22 Å, while the average values of the C=C bond lengths ranged from 1.34 to 1.39 Å, confirming that these are typical double bonds. The lengths of the C–Cl bonds in the compounds were approximately 1.71 Å. The bond lengths between the sp<sup>2</sup>-hybridized C atoms of the benzene and quinoline rings are approximately 1.38 Å, confirming the aromatic character of the rings. While the single bond length between the sp<sup>3</sup>-hybridized methyl carbon and the oxygen atom in the ester group attached to the aromatic benzene ring in the AQQ2 was measured as 1.45 Å, the bond length between the sp<sup>2</sup>-hybridized carbon and the oxygen atom was found to be shorter, 1.33 Å, in agreement with hybridization theory. As

Table 2. Minimum Inhibitory Concentration (MIC) Values of the Aminated QQs (AQQ1–9) for Antibacterial Activity<sup>a</sup>

Aminated QQs		Substituent (R)	Gram-negative Bacteria (MIC, µg/mL)				Gram-positive Bacteria (MIC, µg/mL)		
General Formula	ID		<i>P. aeruginosa</i> (ATCC 27853)	<i>E. coli</i> (ATCC 25922)	<i>K. pneumoniae</i> (ATCC 4352)	<i>P. mirabilis</i> (ATCC 14153)	<i>S. aureus</i> (ATCC 29213)	<i>S. epidermidis</i> (ATCC 12228)	<i>E. faecalis</i> (ATCC 29212)
	AQQ1	2-COOCH <sub>3</sub>	-	-	-	-	1250	-	625
	AQQ2	3-COOCH <sub>3</sub>	-	-	-	-	19.53	625	-
	AQQ3	4-COOCH <sub>3</sub>	-	-	-	-	78.12	625	312.5
	AQQ4	2-COOCH <sub>2</sub> CH <sub>3</sub>	625	-	-	-	156.25	-	312.5
	AQQ5	3-COOCH <sub>2</sub> CH <sub>3</sub>	-	-	-	-	1250	625	312.5
	AQQ6	4-COOCH <sub>2</sub> CH <sub>3</sub>	-	-	-	-	39.06	156.25	78.12
	AQQ7	2-COOC(CH <sub>3</sub> ) <sub>3</sub>	-	-	-	-	19.53	-	156.25
	AQQ8	3-COOC(CH <sub>3</sub> ) <sub>3</sub>	-	-	-	-	4.88	-	156.25
	AQQ9	4-COOC(CH <sub>3</sub> ) <sub>3</sub>	-	-	-	-	2.44	-	78.12
Ciprofloxacin			0.125	0.007	0.125	0.007	0.25	0.25	0.25

<sup>a</sup>“-” means no activity.

Table 3. Minimum Inhibitory Concentration (MIC) Values of the Aminated QQs (AQQ1–9) for Antifungal Activity<sup>a</sup>

Aminated QQs		Substituent (R)	Fungi (MIC, µg/mL)		
General Formula	ID		<i>C. albicans</i> (ATCC 10231)	<i>C. parapsilosis</i> (ATCC 22019)	<i>C. tropicalis</i> (ATCC 750)
	AQQ1	2-COOCH <sub>3</sub>	-	-	625
	AQQ2	3-COOCH <sub>3</sub>	312.5	156.25	312.5
	AQQ3	4-COOCH <sub>3</sub>	78.12	78.12	156.25
	AQQ4	2-COOCH <sub>2</sub> CH <sub>3</sub>	156.25	78.12	156.25
	AQQ5	3-COOCH <sub>2</sub> CH <sub>3</sub>	156.25	156.25	-
	AQQ6	4-COOCH <sub>2</sub> CH <sub>3</sub>	312.50	156.25	625
	AQQ7	2-COOC(CH <sub>3</sub> ) <sub>3</sub>	-	-	-
	AQQ8	3-COOC(CH <sub>3</sub> ) <sub>3</sub>	312.5	156.25	312.5
	AQQ9	4-COOC(CH <sub>3</sub> ) <sub>3</sub>	312.5	156.25	-
Clotrimazole			4.9	-	-
Amphotericin B			-	0.5	1

<sup>a</sup>“-” means no activity.

expected, the strong carbon–oxygen double bond was shortened, with a length of 1.19 Å (Table S1 in the Supporting Information). The C–C–C angles of the benzoquinone, pyridine, and benzene rings and C–C–O angles of the benzoquinone ring in compounds were very close to 120.8°, which supports the structures involving sp<sup>2</sup>-hybridized atoms. It is known that methyl groups generally adopt an ideal tetrahedral geometry with H–C–H and C–C–H bond angles of 109.5°, and the angles of the methyl group in compounds are observed at 109.5° (Table S2 in the Supporting Information). The torsion angles of compounds were given in Table S3 in the Supporting Information. The crystal structures of the QQ and AQQ2 were stabilized by hydrogen bonds formed between the C–H groups as H-bond donors (D) and N, O, or chlorine atoms as H-bond acceptors (A) (Table S4 in the Supporting Information). The C–H···O, C–H···N, and C–H···Cl hydrogen bonds are moderately strong, as their H···A distances cover the range of 2.44–2.88 Å. All parameters of the hydrogen bonds are shown in Table S4 in the Supporting Information.

**2.2. Biological Activity.** **2.2.1. Determination of Minimum Inhibitory Concentrations (MIC) and Structure–Activity Relationship (SAR) Study.** Initially, the antimicrobial profile of the aminated QQs was determined *in vitro* using a minimum inhibitory concentration (MIC) assay against Gram-negative and Gram-positive bacterial strains in addition to yeast strains to determine the lowest concentration capable of inhibiting growth. Prior to the biological test, the purity of the

aminated QQs was confirmed by HPLC with hexane/2-propanol = 95:5 as the mobile phase at a flow rate of 1.0 mL/min. The purity of all aminated QQs was ≥95%. Their chromatograms are provided in the Supporting Information (Figures S2–S10). The MIC values listed in Tables 2 and 3 were compared with those of the commercially available broad-spectrum reference drug ciprofloxacin. The MIC values revealed that all of the aminated QQs did not show antibacterial activity against Gram-negative (*P. aeruginosa*, *E. coli*, *K. pneumoniae*, and *P. mirabilis*) strains. Most of the aminated QQs displayed a moderate activity against Gram-positive bacterial strains, some with MIC values as low as 19.53 µg/mL. Overall, the two aminated QQs (AQQ8 and AQQ9) had the most promising antibacterial profiles against *S. aureus* and *E. faecalis*. In particular, the MIC values of the aminated QQs (AQQ8 and AQQ9), with 4.88 and 2.44 µg/mL, respectively, were 10- to 20-fold higher than the broad-spectrum reference drug ciprofloxacin against *S. aureus*. The two aminated QQs (AQQ6 and AQQ9) were active against *E. faecalis* with MIC value of 78.12 µg/mL. Furthermore, AQQ7 and AQQ8 showed low potency against *E. faecalis* with a MIC value of 156.25 µg/mL. In the analysis of antifungal activity, AQQ3 and AQQ4 were the most potent, with MIC value of 78.12 µg/mL against *C. albicans* and *C. parapsilosis*. Based on the standard MIC results, we also aimed to determine the potential antimicrobial activities of selected active molecules (AQQ8 and AQQ9) against clinically obtained methicillin-resistant strains of *S. aureus*. The *in vitro* activities of AQQ8

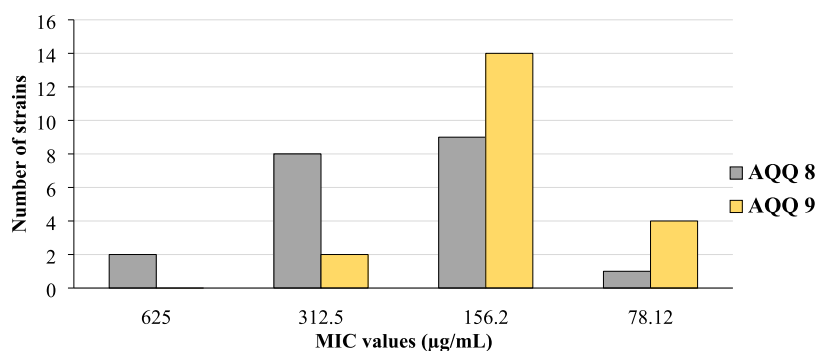


Figure 4. MIC distribution of AQQ8 and AQQ9 against 20 clinically obtained methicillin-resistant *S. aureus* isolates.

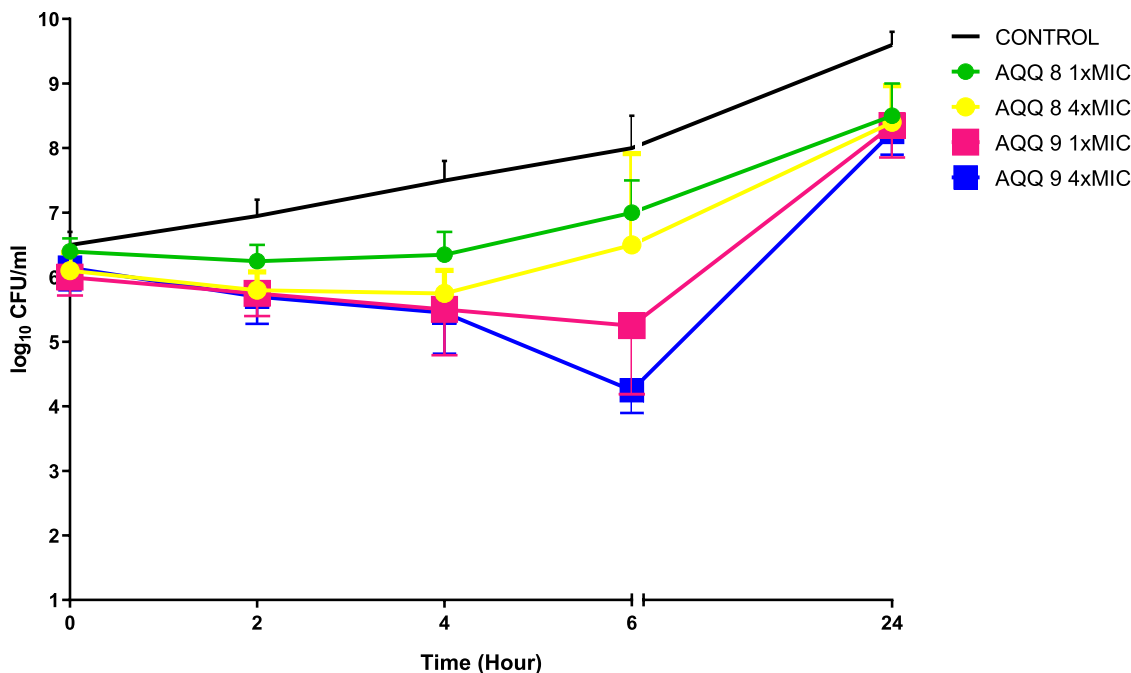


Figure 5. Time-kill determinations for MRSA after treatment with AQQ8 and AQQ9 at 1× and 4× MIC, respectively. The *x*-axis represents the killing time, and the *y*-axis represents the logarithmic MRSA survival, respectively.

and AQQ9 against 20 clinical isolates of MRSA are summarized in Figure 4 (the MIC distribution of levofloxacin as a reference drug against these *S. aureus* strains is also provided in the Supporting Information (Figure S1)). Although the *in vitro* activity of AQQ9 was found to be moderate against the studied strains, neither AQQ8 nor AQQ9 was as active against the MRSA isolates as the standard ATCC strain.

We investigated the replacement of the substituent in three positions on the aminophenyl moiety while maintaining the QQ moiety. We analyzed the SAR study to understand the effect of the substituent in different positions. In general, we could deduce from the SAR that an increase in inhibitory activity was observed when the length of the alkyl chain attached to an ester group in the aminophenyl moiety was changed from a methyl to an ethyl or a *tert*-butyl group. The SAR study demonstrated that the ester group, in particular, with a branched alkyl chain ( $-\text{COOC}(\text{CH}_3)_3$ ) at the 3- or 4-position in the ring (AQQ8 and AQQ9) increased the antibacterial activity against *S. aureus* and *E. faecalis* strains. Moreover, when the branched alkyl chain was replaced with an unbranched alkyl chain ( $\text{COOCH}_2\text{CH}_3$ ), the corresponding

AQQ (AQQ6) displayed a similar level of antibacterial activity against *E. faecalis*. The shift of the ester group with a branched alkyl chain from positions 2- to 3- or 3- to 4- improved the antibacterial activity against *S. aureus* and *E. faecalis*.

**2.2.2. Time-Kill Kinetic Study.** AQQ8 and AQQ9 were selected for further analysis of the mode of action after *in vitro* antimicrobial activity analysis. Time-kill kinetic (TKK) studies for AQQ8 and AQQ9 were performed on one clinically obtained methicillin-resistant *S. aureus*, and the results are given in Figure 5.

The results of the TKK studies did not reveal any bactericidal activity (with a 3  $\log_{10}$  kill determined) for the studied strain at 1× and 4× MIC concentrations within 24 h (Figure 6). When 4× MIC concentration was used for AQQ9, we observed 2  $\log_{10}$  reductions in viable cell count at 6 h; however, regrowth was seen within 24 h. There was only 1  $\log_{10}$  reduction of the viable microorganism cell count within 24 h compared to control for the two tested molecules at all of the studied concentrations.

**2.2.3. Evaluation of the In Vitro Antibiofilm Activity.** Microorganisms attach to surfaces and develop biofilms. These cells are embedded in extracellular polymeric substances, a

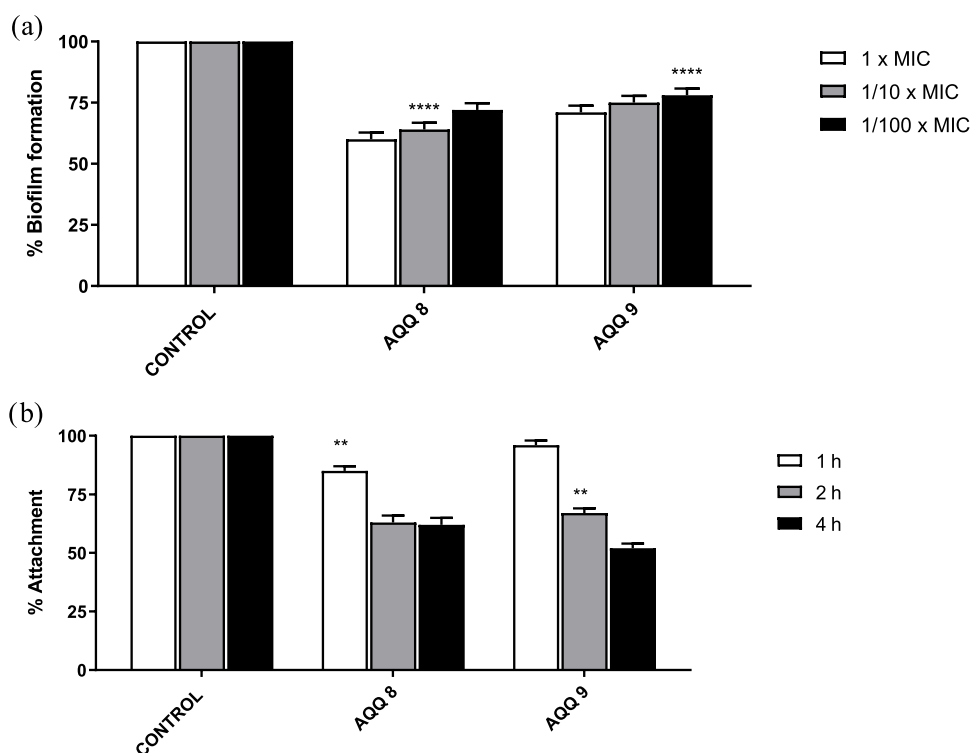
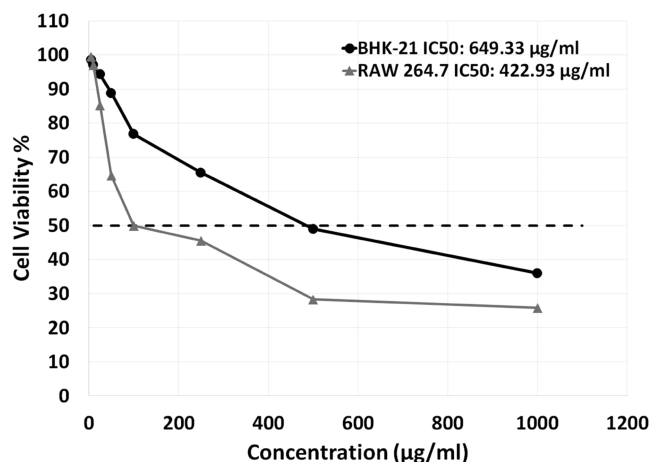


**Figure 6.** Inhibition of *MRSA* biofilms; (a) biofilm formation in each well containing 1 $\times$ , 1/10 $\times$ , and 1/100 $\times$  MIC of the compound and an inoculum of  $1 \times 10^6$ – $1 \times 10^7$  CFU/200  $\mu$ L, incubated for 24 h at 37  $^{\circ}$ C for *MRSA*, (b) surface attachment to the wells contained 1/10 $\times$  MIC of molecules and an inoculum of  $1 \times 10^6$  CFU/200  $\mu$ L, incubated for 1, 2, and 4 h at 37  $^{\circ}$ C for *MRSA*. Control bars indicate wells with microorganisms without containing the test compounds (100% activity). Six wells were used for the tested molecules. Each experiment is representative of two independent tests. All differences between the control and biofilms treated with test compounds were statistically significant (\*\*\*\* $p < 0.0001$ ; \*\* $p = 0.0067$ ).

matrix generally composed of DNA, proteins, and polysaccharides, which are highly resistant to antibiotics. It is one of the major causes of infection persistence, especially in nosocomial settings through indwelling devices. Approximately up to 60% of recurrent microbial infections in the human body are due to bacterial biofilm. Microbial cells within biofilms have shown 10–1000 times more antimicrobial resistance than their planktonic counterparts. Successful treatment of biofilm-associated infections is challenging due to high antimicrobial resistance in these bacterial communities. Classical antibiotics chemotherapy cannot completely eradicate bacterial cells embedded in the biofilm and leads to the emergence of a worsening situation globally. Therefore, to overcome the drug resistance of bacterial biofilm communities; alternative strategies and novel antibiofilm agents are being investigated.<sup>30</sup>

Among the tested QQs, two AQQs (AQQ8 and AQQ9) showed antibacterial activity against *MRSA*. Thus, we mainly focused on these two AQQs for further biofilm inhibition assay. For this purpose, the 1/10 $\times$  MICs of tested effective AQQ8 and AQQ9 molecules were examined for 1, 2, and 4 h at 37  $^{\circ}$ C for *MRSA*'s adherence to the wells of tissue culture microtiter plates. The tested agents inhibited biofilm attachment by nearly 50%. Inhibition rates of adhesion showed a time-dependent effect for the tested molecules. Upon evaluating the % biofilm formation of the studied strains, the rates of biofilm formation inhibition were found to be affected by the tested concentrations with a little difference; the highest inhibition rates were observed at 1 $\times$  MICs for the tested molecules, as expected (Figure 6).

**2.2.4. Cytotoxicity Assays.** To evaluate the selectivity, the cytotoxicity of AQQ8 was examined in two different noncancer and cancer cell lines. In the BHK-21 cell line, AQQ8 showed an IC<sub>50</sub> value of 649.33  $\mu$ g/mL (Figure 7), while the reference

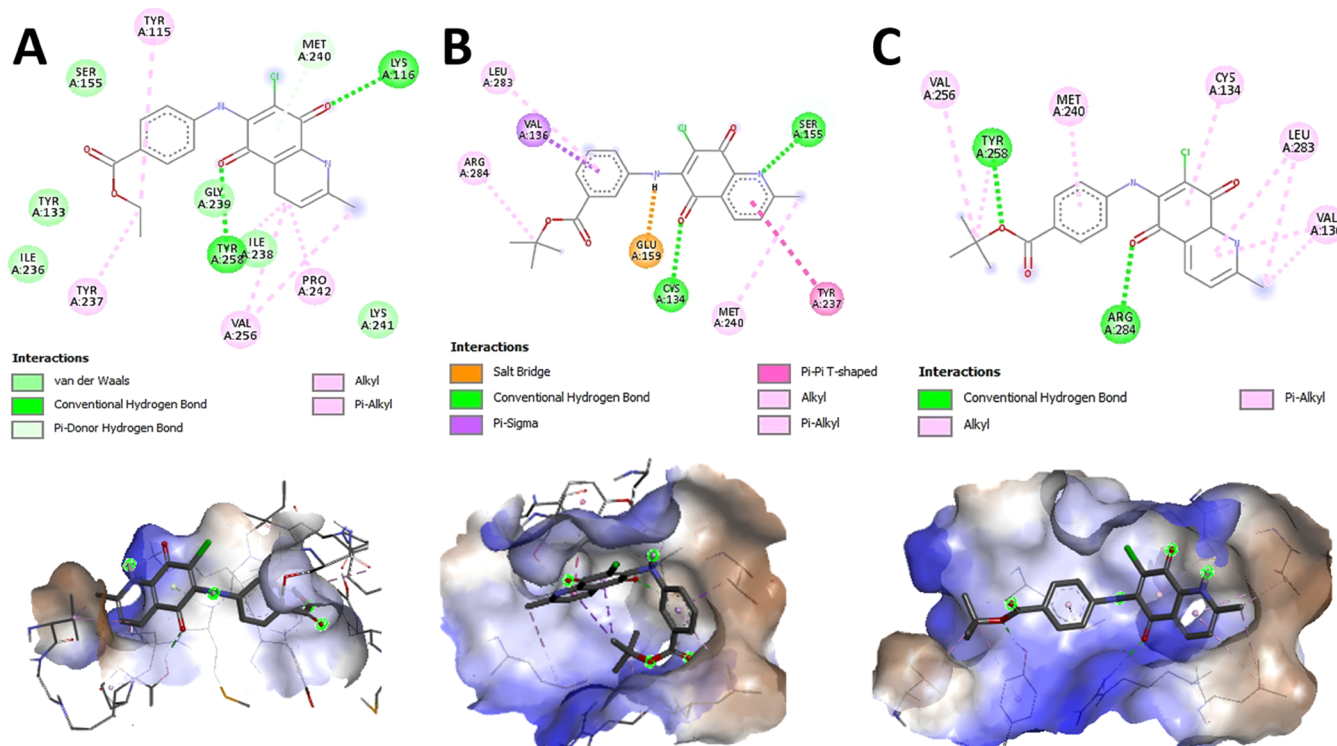


**Figure 7.** Effect of the AQQ8 on the % cell viability at different concentrations.

drug favipiravir has a 1571.04  $\mu$ g/mL IC<sub>50</sub> value. Also, in cancer cell line (RAW 264.7), IC<sub>50</sub> was determined as 422.93  $\mu$ g/mL for AQQ8 (Figure 7), while for the reference drug favipiravir, it is 451.35  $\mu$ g/mL. AAQ8 has a similar inhibition to reference drug on cancer cell line, while the inhibitory potency of this analogue is lower for the reference drug.

**Table 4. Summary of Molecular Docking Studies for AQQ6, AQQ8, and AQQ9 against the Two Protein Targets as Analyzed Using the PLIP**

protein	compound	binding energy (kcal/mol)	H-bonds	hydrophobic interactions
thioredoxin reductase (TrxR) (AFQ6GIM7)	AQQ6	-7.04	2 (LYS116, TYR258)	7 (2*TYR115, TYR133, TYR237, MET240, VAL256, TYR258)
	AQQ8	-7.44	4 (SER155, CYS134, GLU159, ARG284, GLN285)	4 (TYR115, VAL136, LEU283, ARG284)
	AQQ9	-6.89	3 (TYR115, 2*ARG284)	3 (TYR115, VAL136, MET240)
polynucleotide phosphorylase (AFQ6GHG1)	AQQ6	-8.04	1 (PHE103)	7 (2*ARG100, 2*PRO101, LYS105, ILE513, LYS514)
	AQQ8	-9.45	4 (PHE103, GLY106, GLN146, LYS514)	5 (PHE57, PHE103, PRO104, 2*LYS105)
	AQQ9	-8.07	2 (PHE103, ILE513)	4 (ARG100, PRO101, LYS105, LYS514)

**Figure 8.** Schematic 2D and 3D representation of protein–ligand interactions between the key residues of thioredoxin reductase 1 from *S. aureus* (strain MRSA252) (AlphaFold ID: AFQ6GIM7) and (A) AQQ6, (B) AQQ8, and (C) AQQ9.

**2.2.5. In Silico Molecular Docking Studies.** A summary of key results from the docking study is provided in Table 4. We selected the top ligands (AQQ6 and AQQ9) against *S. aureus* and (AQQ8 and AQQ9) against *E. faecalis* strains, and then performed molecular docking against the two target proteins to further predict their activity against these targets.

All three compounds (AQQ6, AQQ8, and AQQ9) appeared to form stronger binding interactions with the active pocket residues of TrxR (Table 4). AQQ8 and AQQ9 also showed interactions with residues between 134 and 137, which is the redox-active region for this protein (Figure 8).

The activity profile of all three molecules (AQQ6, AQQ8, and AQQ9) against PNPase was similar to that for TrxR, with significantly favorable binding energies (−8.04, −9.45, and −8.07 kcal/mol, respectively) (Table 4). Both AQQ8 and AQQ9 showed interactions with LYS514. AQQ8 formed four hydrogen bonds with the residues from the active site of the protein, explaining the high docking score (Figure 9).

Overall, AQQ8 appeared to have the most favorable activity profile in both proteins, with strong hydrogen bonding. As noted in the SAR studies, an increase in the length of the alkyl chain on the aminophenyl group appears to improve the activity, as demonstrated by the docking scores.

### 3. CONCLUSIONS

In summary, we have successfully reported the synthesis and *in vitro* antimicrobial activity determination of the aminated QQs (AQQ1–9) containing an ester group in aryl amine obtained from the amination of QQ, synthesized by chlorooxidation of 8-hydroxy-2-methyl-quinoline (HQ) with sodium chlorate in concentrated HCl solution, with the corresponding aryl amines in the presence of the Lewis acid as a catalyst. Among these aminated QQs, two aminated QQs (AQQ8 and AQQ9) showed promising antibacterial profiles against Gram-positive strains (*S. aureus*) with MIC values 10- to 20-fold less than the reference drug, ciprofloxacin. Based on these results, the two aminated QQs (AQQ8 and AQQ9) were further tested to

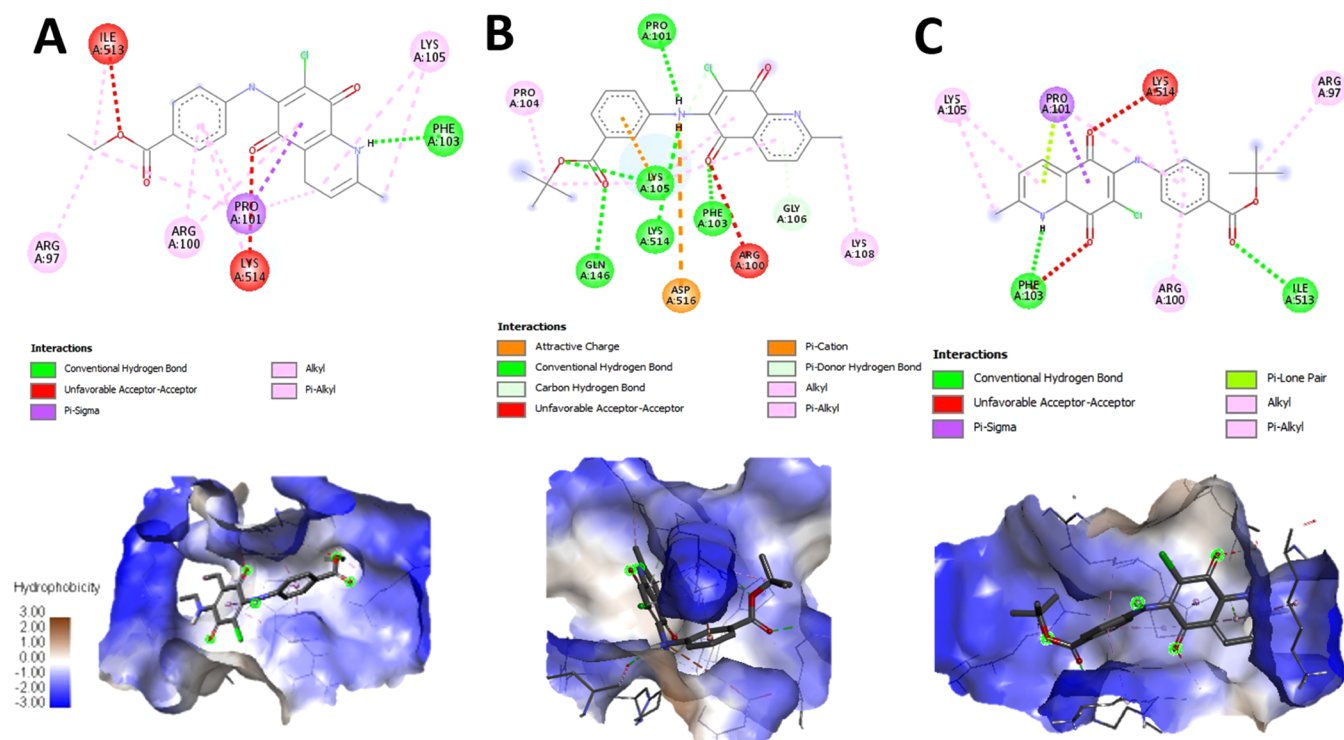


**Figure 9.** Schematic 2D representation of protein–ligand interactions between the key residues of polynucleotide phosphorylase (PNPase) from *S. aureus* (strain MRSA252) (AlphaFold ID: AFQ6GHG1) and (A) AQQ6, (B) AQQ8, and (C) AQQ9.

explore the antibacterial potential in terms of their antibiofilm activity against *MRSA*, and the time-kill kinetic study was performed to assess bactericidal potential. To the best of our knowledge, our study is the first to evaluate the antibiofilm and bactericidal activities of the aminated QQs against clinical *MRSA* isolates. According to our results, AQQ9 was effective against the tested clinical strains with a MIC<sub>90</sub> value of 156.25 μg/mL. According to the initial results from the time-kill curve studies in the present study, this molecule effectively inhibited bacterial growth against methicillin-resistant *S. aureus* isolates within 6 h when used at 4-fold the MIC concentration (over 2 log<sub>10</sub> reduction in viable cell count). As a result, AQQ9 was considered an option for further studies, potentially as a combination therapy against infections caused by clinically resistant *Staphylococcus* spp. Eliminating biofilm from the surfaces is challenging because of the strong antimicrobial resistance. Nearly 50% reduction in the attachment of the cells to *MRSA* biofilms by AQQ8 and AQQ9 observed in our study suggests that the molecules have promising antibiofilm activity, and these should be considered for future exploration. In conclusion, the antibacterial activity and cytotoxicity of the aminated QQs (AQQ1–9) should encourage researchers to explore them as potential novel drugs.

## 4. EXPERIMENTAL SECTION

**4.1. Chemicals and Apparatus.** All starting materials and chemicals used in this study were purchased from various commercial sources with a minimum purity of 95% and used without further purification. Chemical reactions were monitored by thin-layer chromatography (TLC) (Merck DC-plates, aluminum-based, TLC Silica gel 60 F<sub>254</sub>) purchased from Merck KGaA, and plates were visualized using UV light (254 nm). All compounds were purified by column chromatography with a Silica gel 60 (63–200 μm particle-sized) purchased

from Merck with an appropriate solvent system as eluents. Melting points (mp) were measured in the capillary tube at an electrical melting point (Büchi B-540) and are uncorrected. <sup>1</sup>H NMR spectra were recorded at 500 MHz frequency and <sup>13</sup>C NMR spectra were recorded at 125 MHz frequency in the specified deuterated solvent, respectively. Chemical shifts were signified in parts per million (ppm) in CDCl<sub>3</sub> or DMSO-*d*<sub>6</sub> and coupling constants (*J*) are in hertz (Hz). FTIR spectra were recorded using an Alpha T FTIR spectrometer with a single reflection diamond ATR module. High-resolution mass spectra electrospray ionization (HRMS-ESI) was carried out using a Waters SYNAPT G1 MS. Purity of the compounds was further confirmed to be ≥95% by HPLC analyses with Shimadzu/DGU-20A5 HPLC apparatus fitted with a 25 cm Chiralpac AD-H chiral column. The precursor, 6,7-dichloro-2-methyl-5,8-quinolinequinone, QQ, was synthesized using the reported method in the literature.<sup>25</sup>

**4.2. X-ray Diffraction Analysis.** Data for the single-crystal compounds were obtained with Bruker APEX II QUAZAR three-circle diffractometer. Indexing was performed using APEX2.<sup>31</sup> Data integration and reduction were performed using SAINT.<sup>32</sup> Absorption corrections were performed by the multiscan method implemented in SADABS.<sup>33</sup> The Bruker SHELXTL<sup>34</sup> software package was used for structure solution and structure refinement. Crystal structure validations and geometrical calculations were performed using the Platon software.<sup>35</sup> Mercury software<sup>36</sup> was used to visualize the .cif files. The crystallographic and structure refinement data are summarized in Table 1. The selected bond lengths, bond angles, torsion angles, hydrogen-bond distances, and angles are given in the Supporting Information. The crystallographic data have been deposited at the Cambridge Crystallographic Data Centre, and CCDC reference numbers are 2132349 and 2132350 for QQ and AQQ2, respectively. The data can be

retrieved free of charge from <http://www.ccdc.cam.ac.uk/conts/retrieving.html> or from the Cambridge Crystallographic Data Centre (CCDC), 12 Union Road, Cambridge CB2 1EZ, UK; fax: +44 (0)1223336033; email: [deposit@ccdc.cam.ac.uk](mailto:deposit@ccdc.cam.ac.uk).

**4.3. Procedure for the Synthesis of the Methyl Quinolinequinone (QQ).** 4.3.1. 6,7-Dichloro-2-methyl-5,8-quinolinequinone (QQ).<sup>25</sup> 6,7-Dichloro-2-methyl-5,8-quinolinequinone (QQ) was prepared according to the literature from 8-hydroxy-2-methyl-quinoline and sodium chlorate in concentrated HCl in 12% yield. mp 179–180 °C (lit. 180–181 °C). <sup>1</sup>H NMR (500 MHz, CDCl<sub>3</sub>) δ (ppm): 8.31 (d, *J* = 8.10 Hz, 1H, CH<sub>aromatic</sub>), 7.53 (d, *J* = 8.10 Hz, 1H, CH<sub>aromatic</sub>), 2.72 (s, 3H, CH<sub>3</sub>). <sup>13</sup>C NMR (125 MHz, CDCl<sub>3</sub>) δ (ppm): 174.6, 173.5 (>C=O), 165.1, 145.3, 142.9, 141.8, 134.6, 127.2, 125.2 (C<sub>aromatic</sub> and C<sub>q</sub>), 24.3 (CH<sub>3</sub>). MS (+ESI) *m/z* (%): 242 (100, [M + H]<sup>+</sup>), 240 (11, [M - H]<sup>+</sup>). Anal. calcd for C<sub>10</sub>H<sub>5</sub>Cl<sub>2</sub>NO<sub>2</sub> (240.97).

**4.4. General Procedure for the Synthesis of the Aminated Quinolinequinones (AQQ1–9).** A suspension of the QQ (0.250 g, 1.03 mmol) and CeCl<sub>3</sub>·7H<sub>2</sub>O (0.421 g, 1.13 mmol, 1.1 equiv) in ethanol was stirred at room temperature for 1 h. Subsequently, to this solution of the QQ and CeCl<sub>3</sub>·7H<sub>2</sub>O, the corresponding amine (1.13 mmol, 1.1 equiv) in ethanol was successively added and stirred for 3–16 h until QQ was completely consumed. After evaporating the solvent, the residue was dissolved with CH<sub>2</sub>Cl<sub>2</sub> (50 mL), and the solution was washed sequentially with water (3 × 30 mL). The organic layer was dried over CaCl<sub>2</sub>, filtered, and concentrated under reduced pressure. The reaction crude was purified on a silica gel column chromatography using the eluent system to give the corresponding AQQ.

**4.4.1. Methyl 2-((7-chloro-2-methyl-5,8-dioxo-5,8-dihydroquinolin-6-yl)amino)benzoate (AQQ1).** Obtained from the mixture (QQ and CeCl<sub>3</sub>·7H<sub>2</sub>O) and methyl 2-aminobenzoate (0.171 g, 1.13 mmol) according to the general procedure, the title compound (AQQ1) was purified by column chromatography as a dark red solid. Yield: 17%, 260–262 °C. FTIR (ATR) *v* (cm<sup>-1</sup>): 3242 (NH), 3081 (CH<sub>aromatic</sub>), 2959 (CH<sub>aliphatic</sub>), 1682, 1673 (>C=O), 1603, 1570, 1509, 1437, 1317, 1265, 1221, 1189, 1162, 1143, 1089, 1032. <sup>1</sup>H NMR (500 MHz, CDCl<sub>3</sub>) δ (ppm): 10.15 (br s, 1H, NH), 8.36 (d, *J* = 6.7 Hz, 1H, CH<sub>aromatic</sub>), 8.03 (d, *J* = 7.5 Hz, 1H, CH<sub>aromatic</sub>), 7.57–7.48 (m, 2H, CH<sub>aromatic</sub>), 7.16 (t, *J* = 7.3 Hz, 1H, CH<sub>aromatic</sub>), 6.85 (d, *J* = 7.6 Hz, 1H, CH<sub>aromatic</sub>), 3.99 (s, 3H, OCH<sub>3</sub>), 2.82 (s, 3H, CH<sub>3</sub>). <sup>13</sup>C NMR (125 MHz, CDCl<sub>3</sub>) δ (ppm): 179.8, 176.2, 167.9 (>C=O), 165.9, 147.7, 140.4, 139.1, 135.1, 132.4, 130.9, 127.1, 125.2, 123.1, 123.0, 119.4, 118.7 (C<sub>aromatic</sub> and C<sub>q</sub>), 52.5 (OCH<sub>3</sub>), 29.7 (CH<sub>3</sub>). HRMS (+ESI) *m/z* calcd for C<sub>18</sub>H<sub>14</sub>ClN<sub>2</sub>O<sub>4</sub> [M + H]<sup>+</sup>: 357.0642; found: 357.0641.

**4.4.2. Methyl 3-((7-chloro-2-methyl-5,8-dioxo-5,8-dihydroquinolin-6-yl)amino)benzoate (AQQ2).** Obtained from the mixture (QQ and CeCl<sub>3</sub>·7H<sub>2</sub>O) and methyl 3-aminobenzoate (0.171 g, 1.13 mmol) according to the general procedure, the title compound (AQQ2) was purified by column chromatography as an orange solid. Yield: 56%, 196–197 °C. FTIR (ATR) *v* (cm<sup>-1</sup>): 3334 (NH), 3100, 3063 (CH<sub>aromatic</sub>), 2956 (CH<sub>aliphatic</sub>), 1721, 1667 (>C=O), 1579, 1493, 1442, 1427, 1385, 1298, 1281, 1239, 1220, 1180, 1144, 1101, 1038. <sup>1</sup>H NMR (500 MHz, CDCl<sub>3</sub>) δ (ppm): 8.24 (d, *J* = 7.9 Hz, 1H, CH<sub>aromatic</sub>), 7.82 (d, *J* = 7.7 Hz, 1H, CH<sub>aromatic</sub>), 7.68 (s, 1H, CH<sub>aromatic</sub>), 7.61 (br s, 1H, NH), 7.43 (d, *J* = 7.9 Hz, 1H, CH<sub>aromatic</sub>), 7.37 (t, *J* = 7.8 Hz, 1H, CH<sub>aromatic</sub>), 7.23–

7.16 (m, 1H, CH<sub>aromatic</sub>), 3.85 (s, 3H, OCH<sub>3</sub>), 2.72 (s, 3H, CH<sub>3</sub>). <sup>13</sup>C NMR (125 MHz, CDCl<sub>3</sub>) δ (ppm): 179.9, 176.1, 166.3 (>C=O), 166.2, 147.9, 140.7, 137.5, 135.0, 130.7, 128.6, 128.4, 127.0, 126.8, 125.0, 124.7, 116.6 (C<sub>aromatic</sub> and C<sub>q</sub>), 52.4 (OCH<sub>3</sub>), 25.5 (CH<sub>3</sub>). HRMS (+ESI) *m/z* calcd for C<sub>18</sub>H<sub>13</sub>ClN<sub>2</sub>O<sub>4</sub> [M]<sup>+</sup>: 356.0564; found: 356.0565.

**4.4.3. Methyl 4-((7-chloro-2-methyl-5,8-dioxo-5,8-dihydroquinolin-6-yl)amino)benzoate (AQQ3).** Obtained from the mixture (QQ and CeCl<sub>3</sub>·7H<sub>2</sub>O) and methyl 4-aminobenzoate (0.171 g, 1.13 mmol) according to the general procedure, the title compound (AQQ3) was purified by column chromatography as a red solid. Yield: 77%, 261–262 °C. FTIR (ATR) *v* (cm<sup>-1</sup>): 3325 (NH), 3078 (CH<sub>aromatic</sub>), 2959 (CH<sub>aliphatic</sub>), 1701, 1673 (>C=O), 1574, 1522, 1440, 1416, 1297, 1256, 1221, 1197, 1179, 1143, 1121, 1099, 1034. <sup>1</sup>H NMR (500 MHz, DMSO-*d*<sub>6</sub>) δ (ppm): 9.55 (br s, 1H, NH), 8.29 (d, *J* = 8.0 Hz, 1H, CH<sub>aromatic</sub>), 7.88 (d, *J* = 8.6 Hz, 2H, CH<sub>aromatic</sub>), 7.68 (d, *J* = 8.0 Hz, 1H, CH<sub>aromatic</sub>), 7.19 (d, *J* = 8.6 Hz, 2H, CH<sub>aromatic</sub>), 3.83 (s, 3H, OCH<sub>3</sub>), 2.67 (s, 3H, CH<sub>3</sub>). <sup>13</sup>C NMR (125 MHz, DMSO-*d*<sub>6</sub>) δ (ppm): 180.2, 176.2, 166.3 (>C=O), 164.7, 147.6, 144.2, 142.5, 135.2, 129.7, 127.5, 126.1, 124.5, 122.5, 119.9 (C<sub>aromatic</sub> and C<sub>q</sub>), 52.4 (OCH<sub>3</sub>), 25.1 (CH<sub>3</sub>). HRMS (+ESI) *m/z* calcd for C<sub>18</sub>H<sub>14</sub>ClN<sub>2</sub>O<sub>4</sub> [M + H]<sup>+</sup>: 357.0642; found: 357.0641.

**4.4.4. Ethyl 2-((7-chloro-2-methyl-5,8-dioxo-5,8-dihydroquinolin-6-yl)amino)benzoate (AQQ4).** Obtained from the mixture (QQ and CeCl<sub>3</sub>·7H<sub>2</sub>O) and ethyl 2-aminobenzoate (0.191 g, 1.13 mmol) according to the general procedure, the title compound (AQQ4) was purified by column chromatography as a red solid. Yield: 38%, 186–188 °C. FTIR (ATR) *v* (cm<sup>-1</sup>): 3241 (NH), 3078 (CH<sub>aromatic</sub>), 2956, 2923, 2856 (CH<sub>aliphatic</sub>), 1729, 1678 (>C=O), 1599, 1571, 1511, 1450, 1367, 1307, 1258, 1223, 1141, 1088. <sup>1</sup>H NMR (500 MHz, CDCl<sub>3</sub>) δ (ppm): 10.16 (br s, 1H, NH), 8.34 (d, *J* = 7.2 Hz, 1H, CH<sub>aromatic</sub>), 8.03 (d, *J* = 7.5 Hz, 1H, CH<sub>aromatic</sub>), 7.57–7.44 (m, 2H, CH<sub>aromatic</sub>), 7.15 (t, *J* = 7.1 Hz, 1H, CH<sub>aromatic</sub>), 6.84 (d, *J* = 7.5 Hz, 1H, CH<sub>aromatic</sub>), 4.51–4.32 (m, 2H, OCH<sub>2</sub>), 2.81 (s, 3H, CH<sub>3</sub>), 1.45 (t, *J* = 6.7 Hz, 3H, CH<sub>3</sub>). <sup>13</sup>C NMR (125 MHz, CDCl<sub>3</sub>) δ (ppm): 179.8, 176.2, 167.4 (>C=O), 165.9, 147.7, 140.5, 139.0, 135.1, 132.2, 130.9, 127.1, 125.2, 123.0, 123.0, 119.2, 119.1 (C<sub>aromatic</sub> and C<sub>q</sub>), 61.6 (OCH<sub>2</sub>), 25.5, 14.3 (CH<sub>3</sub>). HRMS (+ESI) *m/z* calcd for C<sub>19</sub>H<sub>16</sub>ClN<sub>2</sub>O<sub>4</sub> [M + H]<sup>+</sup>: 371.0799; found: 371.0795.

**4.4.5. Ethyl 3-((7-chloro-2-methyl-5,8-dioxo-5,8-dihydroquinolin-6-yl)amino)benzoate (AQQ5).** Obtained from the mixture (QQ and CeCl<sub>3</sub>·7H<sub>2</sub>O) and ethyl 3-aminobenzoate (0.191 g, 1.13 mmol) according to the general procedure, the title compound (AQQ5) was purified by column chromatography as an orange solid. Yield: 49%, 167–168 °C. FTIR (ATR) *v* (cm<sup>-1</sup>): 3326 (NH), 3085 (CH<sub>aromatic</sub>), 2981, 2937, 2904 (CH<sub>aliphatic</sub>), 1713, 1666 (>C=O), 1603, 1579, 1508, 1470, 1446, 1365, 1306, 1281, 1248, 1219, 1197, 1165, 1144, 1105, 1034. <sup>1</sup>H NMR (500 MHz, CDCl<sub>3</sub>) δ (ppm): 8.33 (d, *J* = 7.7 Hz, 1H, CH<sub>aromatic</sub>), 7.92 (d, *J* = 7.6 Hz, 1H, CH<sub>aromatic</sub>), 7.78 (s, 1H, CH<sub>aromatic</sub>), 7.67 (br s, 1H, NH), 7.51 (d, *J* = 7.8 Hz, 1H, CH<sub>aromatic</sub>), 7.46 (t, *J* = 7.7 Hz, 1H, CH<sub>aromatic</sub>), 7.27 (m, 1H, CH<sub>aromatic</sub>), 4.40 (q, *J* = 7.0 Hz, 2H, OCH<sub>2</sub>), 2.81 (s, 3H, CH<sub>3</sub>), 1.41 (t, *J* = 7.0 Hz, 3H, CH<sub>3</sub>). <sup>13</sup>C NMR (125 MHz, CDCl<sub>3</sub>) δ (ppm): 179.9, 176.1, 166.2 (>C=O), 165.8, 147.9, 140.7, 137.4, 135.0, 131.1, 128.5, 128.3, 127.0, 126.8, 125.0, 124.7, 116.5 (C<sub>aromatic</sub> and C<sub>q</sub>), 61.3 (OCH<sub>2</sub>), 25.5, 14.3 (CH<sub>3</sub>). HRMS (+ESI) *m/z* calcd for C<sub>19</sub>H<sub>15</sub>ClN<sub>2</sub>O<sub>4</sub> [M]<sup>+</sup>: 370.0720; found: 370.0725.

**4.4.6. Ethyl 4-((7-chloro-2-methyl-5,8-dioxo-5,8-dihydroquinolin-6-yl)amino)benzoate (AQQ6).** Obtained from the mixture (QQ and CeCl<sub>3</sub>·7H<sub>2</sub>O) and ethyl 4-aminobenzoate (0.191 g, 1.13 mmol) according to the general procedure, the title compound (AQQ6) was purified by column chromatography as a red solid. Yield: 25%, 227–229 °C. FTIR (ATR)  $\nu$  (cm<sup>-1</sup>): 3222 (NH), 2993, 2944, 2907 (CH<sub>aliphatic</sub>), 1688, 1674 (>C=O), 1576, 1520, 1496, 1474, 1450, 1413, 1367, 1306, 1279, 1258, 1221, 1200, 1171, 1128, 1103, 1036, 1014. <sup>1</sup>H NMR (500 MHz, CDCl<sub>3</sub>)  $\delta$  (ppm): 8.34 (d, *J* = 8.0 Hz, 1H, CH<sub>aromatic</sub>), 8.06 (d, *J* = 8.6 Hz, 2H, CH<sub>aromatic</sub>), 7.70 (br s, 1H, NH), 7.53 (d, *J* = 8.0 Hz, 1H, CH<sub>aromatic</sub>), 7.09 (d, *J* = 8.5 Hz, 2H, CH<sub>aromatic</sub>), 4.40 (q, *J* = 7.1 Hz, 2H, OCH<sub>2</sub>), 2.81 (s, 3H, CH<sub>3</sub>), 1.42 (t, *J* = 7.1 Hz, 3H, CH<sub>3</sub>). <sup>13</sup>C NMR (125 MHz, CDCl<sub>3</sub>)  $\delta$  (ppm): 179.9, 176.1, 166.3 (>C=O), 165.9, 147.8, 141.1, 140.3, 135.0, 130.0, 127.1, 127.1, 124.8, 122.8, 118.0 (C<sub>aromatic</sub> and C<sub>q</sub>), 61.1 (OCH<sub>2</sub>), 25.5, 14.3 (CH<sub>3</sub>). HRMS (+ESI) *m/z* calcd for C<sub>19</sub>H<sub>16</sub>ClN<sub>2</sub>O<sub>4</sub> [M + H]<sup>+</sup>: 371.0799; found: 371.0790.

**4.4.7. tert-Butyl 2-((7-chloro-2-methyl-5,8-dioxo-5,8-dihydroquinolin-6-yl)amino)benzoate (AQQ7).** Obtained from the mixture (QQ and CeCl<sub>3</sub>·7H<sub>2</sub>O) and tert-butyl 2-aminobenzoate (0.218 g, 1.13 mmol) according to the general procedure, the title compound (AQQ7) was purified by column chromatography as an orange solid. Yield: 13%, 194–194.7 °C. FTIR (ATR)  $\nu$  (cm<sup>-1</sup>): 3246 (NH), 3063 (CH<sub>aromatic</sub>), 2975, 2926 (CH<sub>aliphatic</sub>), 1695, 1680 (>C=O), 1571, 1523, 1451, 1365, 1277, 1246, 1224, 1160, 1143, 1108, 1082, 1032. <sup>1</sup>H NMR (500 MHz, CDCl<sub>3</sub>)  $\delta$  (ppm): 10.18 (br s, 1H, NH), 8.37–8.27 (m, 1H, CH<sub>aromatic</sub>), 7.99–7.89 (m, 1H, CH<sub>aromatic</sub>), 7.56–7.40 (m, 2H, CH<sub>aromatic</sub>), 7.18–7.06 (m, 1H, CH<sub>aromatic</sub>), 6.83–6.76 (m, 1H, CH<sub>aromatic</sub>), 2.81 (s, 3H, CH<sub>3</sub>), 1.64 (s, 9H, CH<sub>3</sub>). <sup>13</sup>C NMR (125 MHz, CDCl<sub>3</sub>)  $\delta$  (ppm): 179.9, 176.2, 166.7 (>C=O), 165.8, 147.7, 140.5, 138.7, 135.1, 131.7, 131.1, 127.1, 125.2, 123.0, 120.6, 119.0 (C<sub>aromatic</sub> and C<sub>q</sub>), 82.6 (OC), 28.3, 25.4 (CH<sub>3</sub>). HRMS (+ESI) *m/z* calcd for C<sub>21</sub>H<sub>20</sub>ClN<sub>2</sub>O<sub>4</sub> [M + H]<sup>+</sup>: 399.1112; found: 399.1109.

**4.4.8. tert-Butyl 3-((7-chloro-2-methyl-5,8-dioxo-5,8-dihydroquinolin-6-yl)amino)benzoate (AQQ8).** Obtained from the mixture (QQ and CeCl<sub>3</sub>·7H<sub>2</sub>O) and tert-butyl 3-aminobenzoate (0.218 g, 1.13 mmol) according to the general procedure, the title compound (AQQ8) was purified by column chromatography as a red solid. Yield: 25%, 188.7–189.5 °C. FTIR (ATR)  $\nu$  (cm<sup>-1</sup>): 3189 (NH), 3022 (CH<sub>aromatic</sub>), 2978, 2937 (CH<sub>aliphatic</sub>), 1708, 1685 (>C=O), 1652, 1559, 1516, 1485, 1427, 1368, 1303, 1285, 1222, 1162, 1109, 1042. <sup>1</sup>H NMR (500 MHz, CDCl<sub>3</sub>)  $\delta$  (ppm): 8.35–8.25 (m, 1H, CH<sub>aromatic</sub>), 7.88–7.79 (m, 1H, CH<sub>aromatic</sub>), 7.76–7.64 (m, 2H, NH and CH<sub>aromatic</sub>), 7.53–7.45 (m, 1H, CH<sub>aromatic</sub>), 7.45–7.35 (m, 1H, CH<sub>aromatic</sub>), 7.25–7.16 (m, 1H, CH<sub>aromatic</sub>), 2.79 (s, 3H, CH<sub>3</sub>), 1.60 (s, 9H, CH<sub>3</sub>). <sup>13</sup>C NMR (125 MHz, CDCl<sub>3</sub>)  $\delta$  (ppm): 179.9, 176.1, 166.1 (>C=O), 164.8, 147.9, 140.7, 137.2, 135.0, 132.6, 128.3, 128.0, 126.9, 126.7, 124.8, 124.7, 116.3 (C<sub>aromatic</sub> and C<sub>q</sub>), 81.6 (OC), 28.2, 25.4 (CH<sub>3</sub>). HRMS (+ESI) *m/z* calcd for C<sub>21</sub>H<sub>20</sub>ClN<sub>2</sub>O<sub>4</sub> [M + H]<sup>+</sup>: 399.1112; found: 399.1109.

**4.4.9. tert-Butyl 4-((7-chloro-2-methyl-5,8-dioxo-5,8-dihydroquinolin-6-yl)amino)benzoate (AQQ9).** Obtained from the mixture (QQ and CeCl<sub>3</sub>·7H<sub>2</sub>O) and tert-butyl 4-aminobenzoate (0.218 g, 1.13 mmol) according to the general procedure, the title compound (AQQ9) was purified by column chromatography as a dark red solid. Yield: 35%,

182.5–184.5 °C. FTIR (ATR)  $\nu$  (cm<sup>-1</sup>): 3334 (NH), 3093 (CH<sub>aromatic</sub>), 2959, 2926, 2856 (CH<sub>aliphatic</sub>), 1706, 1666 (>C=O), 1577, 1516, 1496, 1415, 1369, 1285, 1256, 1217, 1160, 1098, 1032. <sup>1</sup>H NMR (500 MHz, CDCl<sub>3</sub>)  $\delta$  (ppm): 8.37–8.28 (m, 1H, CH<sub>aromatic</sub>), 8.05–7.95 (m, 2H, CH<sub>aromatic</sub>), 7.71 (br s, 1H, NH), 7.55–7.48 (m, 1H, CH<sub>aromatic</sub>), 7.10–7.04 (m, 2H, CH<sub>aromatic</sub>), 2.81 (s, 3H, CH<sub>3</sub>), 1.60 (s, 9H, CH<sub>3</sub>). <sup>13</sup>C NMR (125 MHz, CDCl<sub>3</sub>)  $\delta$  (ppm): 179.9, 176.1, 166.2 (>C=O), 165.0, 147.8, 140.7, 140.4, 135.0, 129.9, 128.7, 127.0, 124.8, 122.8, 117.7 (C<sub>aromatic</sub> and C<sub>q</sub>), 81.2 (OC), 28.2, 25.5 (CH<sub>3</sub>). HRMS (+ESI) *m/z* calcd for C<sub>21</sub>H<sub>20</sub>ClN<sub>2</sub>O<sub>4</sub> [M + H]<sup>+</sup>: 399.1112; found: 399.1106.

**4.5. Biological Evaluation.** MICs of the molecules were examined using the broth microdilution technique approved by the Clinical and Laboratory Standards Institute (CLSI).<sup>37,38</sup> The inoculum of the tested four Gram-negative bacteria (*Pseudomonas aeruginosa* ATCC 27853, *Escherichia coli* ATCC 25922, *Klebsiella pneumoniae* ATCC 4352, *Proteus mirabilis* ATCC 14153), three Gram-positive bacteria (*Staphylococcus aureus* ATCC 29213, *Staphylococcus epidermidis* ATCC 12228, *Enterococcus faecalis* ATCC 29212), and three yeast (*Candida albicans* ATCC 10231, *Candida parapsilosis* ATCC 22019, *Candida tropicalis* ATCC 750) species were prepared according to CLSI recommendations. The stock solutions of the tested molecules were prepared in DMSO. Serial twofold dilutions ranging from 1250 to 0.06  $\mu$ g/mL were prepared in Mueller Hinton Broth for the tested bacteria and RPMI-1640 medium for the yeast, respectively.

According to the antimicrobial activity results, we aimed to identify *in vitro* activities of the AQQ8 and AQQ9 against clinically obtained strains using the broth microdilution dilution technique as per the CLSI recommendations.<sup>37,38</sup> For this assay, 20 nonduplicate, nosocomially acquired methicillin-resistant *S. aureus* isolated from blood specimens between April and September 2017 were obtained from the Department of Infectious Diseases and Clinical Microbiology, Faculty of Medicine, Istanbul Medipol University. All strains were identified using API STAPH (bioMérieux SA, Marcy-l'Étoile, France). Next, all of the tested *S. aureus* isolates were chosen using oxacillin susceptibility testing to determine the methicillin-resistant isolates approved by CLSI (MIC  $\geq$  4  $\mu$ g/mL).<sup>37</sup> The MIC was defined as the lowest concentration of tested extracts showing complete inhibition of visible growth. Experiments were performed in triplicate.

**4.5.1. Determination of Time-Kill Curves.** The bactericidal activity of selected molecules (AQQ8 and AQQ9) was assessed using the time-kill curve (TKC) method at 1 and 4 times the MIC against one (1) MRSA clinical strain. The MIC value of the tested strain was 78.12  $\mu$ g/mL for both of the tested molecules. Molecule-free controls were included for the tested strain. Inocula were quantified spectrophotometrically and added to the flasks to yield a final concentration of 1  $\times$  10<sup>6</sup> CFU/mL. The test tubes containing MHB with and without (growth control) molecules in a final volume of 10 mL were incubated in a 37 °C calibrated shaking water bath, and viable counts were determined at 0, 2, 4, 6, and 24 h intervals after inoculation, by subculturing 0.1 mL serial dilutions onto TSA plates. All tests were performed in duplicate. The lower limit of detection for the time-kill assay was 1 log<sub>10</sub> CFU/mL. Bactericidal activity was defined as a  $\geq$  3 log<sub>10</sub> CFU/mL reduction from the initial inoculum.

**4.5.2. Determination of the Antibiofilm Activities.** Biofilm attachment and inhibition of biofilm formation assays were

performed as previously described with some modifications.<sup>39</sup> For biofilm attachment, an overnight culture of strong, biofilm-producing clinically MRSA isolate was diluted 1/50 to obtain  $1 \times 10^6$ – $1 \times 10^7$  CFU/200 mL for bacteria in TSB supplement with 1% glucose. Then, the strain was added to each well of 96-well tissue culture microtiter plates with 1/10× MIC of tested molecules (MIC = 78.12  $\mu$ g/mL). The plates were allowed to incubate for 1, 2, and 4 h at 37 °C. The positive control was studied strain in the medium alone. After incubation, each well was washed with PBS solution three times, and OD was measured at 595 nm.

To inhibit biofilm formation, the tested strain was incubated in its medium and molecules at 1× and 1/10× in addition to 1/100× MIC at 37 °C for 24 h in microtiter plates. Six wells were used for each molecule. The positive control was the tested strain in its medium without molecules. After incubation, each well was washed with PBS solution thrice and OD was measured at 595 nm.

**4.5.3. Cell Culture.** One noncancer cell line and one cancer cell line were used in this study. Baby Hamster kidney cells (BHK-21) and murine macrophage cells from leukemia tumor (RAW 264.7) were from American Type Culture Collection ((ATCC), Manassas, VA). All medium and solutions were heated to 37 °C before the process of cell cultivation. Both cells were cultured in DMEM supplemented with inactivated fetal bovine serum (10%), 1% antibiotic–antimycotic solution in a 37 °C, 5% CO<sub>2</sub> humidified incubator. The monolayer cells in 75 cm<sup>2</sup> cell culture flasks were passaged by trypsinization in the incubator.

**4.5.3.1. Cell Treatments and Cytotoxicity Assay.** For the cytotoxicity assay, cell suspension was seeded in each well ( $1 \times 10^4$  cell) in 96-well microplates and kept in an incubator for 24 h to confluence at least of 90%. The media were replaced with fresh media, and the cells were treated with both compounds with final concentrations of 1000, 500, 250, 100, 50, 25, 10, and 5  $\mu$ g/mL and vehicle control 1% DMSO for 24 h at 37 °C. After 24 h, cell viability was measured using the 3-(4,5-dimethylthiazol2-yl)-2,5-diphenyltetrazolium bromide (MTT) assay. The final volume of the 5 mg/mL MTT reagent was added to the wells, and the plates were incubated in the dark for 3 h. All media was removed and 100  $\mu$ L of DMSO was added to dissolve the formazan crystals. Microplates were read to measure optical density (Absorbance 96, Byonoy, Germany) at 590 nm. Cell viability was expressed as a percentage of the absorbance recorded for vehicle control.

**4.5.4. Statistical Analysis.** All experiments were performed in two independent assays. Two-way ANOVA-Tukey's multiple comparison test was used to compare differences between control and antimicrobials treated biofilms. *p* value < 0.0001 was considered statistically significant.

**4.5.5. Molecular Docking Studies.** All compounds were sketched using PerkinElmer ChemDraw version 21.0 and prepared using Gypsum-DL on Google Colab while applying Durrant lab filters which remove molecular variants that are improbable.<sup>40</sup> Since the target proteins were not available in the Protein Data Bank, the protein structures were obtained from the AlphaFold database. The protein structures obtained from the AlphaFold database were compared with their homologous counterparts from other species available in PDB. Coordinates for cofactor were obtained from other proteins available in the Protein Data Bank, and the same were used to obtain the final structure. The proteins were prepared using UCSF Chimera version 1.4 with all of the default

parameters under the DockPrep module.<sup>41</sup> The conversion of compounds and protein to .pdbqt format, grid preparation, and docking parameter file generation was performed using the scripts available under MGLTools 1.5.7. Molecular docking was performed using AutoDock-GPU with CUDA accelerator and 64 thread block size on Microsoft Azure NC-series VM (Standard\_NC6) powered by the NVIDIA Tesla K80 card and the Intel Xeon E5-2690 v3 (Haswell) processor.<sup>42</sup> The output files were processed using the scripts available under MGLTools 1.5.7, and data visualization was performed using BIOVIA Discovery Studio 2021. Further exploration of the protein–ligand interaction was performed using Protein–Ligand Interaction Profiler (PLIP) 2.2.0 tool.<sup>43</sup>

## ■ ASSOCIATED CONTENT

### Supporting Information

The Supporting Information is available free of charge at <https://pubs.acs.org/doi/10.1021/acsomega.2c03193>.

Details of all crystallographic data of the **QQ** and **AQQ2**, MIC distribution of levofloxacin as a reference drug, purity chromatograms of the aminated **QQs** (**AQQ1–9**), and <sup>1</sup>H and <sup>13</sup>C spectra of the aminated **QQs** (**AQQ1–9**) (PDF)

## ■ AUTHOR INFORMATION

### Corresponding Author

Amaç Fatih TuYUN – Department of Chemistry, Faculty of Science, Istanbul University, 34126 Istanbul, Turkey; [orcid.org/0000-0001-5698-1109](https://orcid.org/0000-0001-5698-1109); Phone: +90212 440 0000; Email: [aftuyun@gmail.com](mailto:aftuyun@gmail.com), [aftuyun@istanbul.edu.tr](mailto:aftuyun@istanbul.edu.tr)

### Authors

Hatice Yıldırım – Department of Chemistry, Engineering Faculty, Istanbul University-Cerrahpasa, 34320 Istanbul, Turkey

Nilüfer Bayrak – Department of Chemistry, Engineering Faculty, Istanbul University-Cerrahpasa, 34320 Istanbul, Turkey

Mahmut Yıldız – Department of Chemistry, Gebze Technical University, 41400 Kocaeli, Turkey; [orcid.org/0000-0001-6317-5738](https://orcid.org/0000-0001-6317-5738)

Emel Mataracı-Kara – Department of Pharmaceutical Microbiology, Pharmacy Faculty, Istanbul University, 34116 Istanbul, Turkey

Serol Korkmaz – Institute of Health Sciences, Marmara University, 34722 Istanbul, Turkey

Deepak Shikhar – Department of Pharmaceutical Sciences & Technology, Birla Institute of Technology, Ranchi 835 215 Jharkhand, India; [orcid.org/0000-0003-1882-1731](https://orcid.org/0000-0003-1882-1731)

Venkatesan Jayaprakash – Department of Pharmaceutical Sciences & Technology, Birla Institute of Technology, Ranchi 835 215 Jharkhand, India; [orcid.org/0000-0002-9724-4153](https://orcid.org/0000-0002-9724-4153)

Complete contact information is available at: <https://pubs.acs.org/10.1021/acsomega.2c03193>

### Notes

The authors declare no competing financial interest.

## ACKNOWLEDGMENTS

This work was financially supported by the Scientific Research Projects Coordination Unit of Istanbul University (project numbers: FBG-2022-38594) and the Scientific Research Projects Coordination Unit of Istanbul University-Cerrahpasa (project numbers: FBA-2019-32249) for supplying the equipment and materials.

## REFERENCES

- (1) Lai, C.-C.; Chen, S.-Y.; Ko, W.-C.; Hsueh, P.-R. Increased antimicrobial resistance during the COVID-19 pandemic. *Int. J. Antimicrob. Agents* **2021**, *57*, No. 106324.
- (2) Knight, G. M.; Glover, R. E.; McQuaid, C. F.; Olaru, I. D.; Gallandat, K.; Leclerc, Q. J.; Fuller, N. M.; Willcocks, S. J.; Hasan, R.; van Kleef, E.; Chandler, C. I. Antimicrobial resistance and COVID-19: Intersections and implications. *eLife* **2021**, *10*, No. e64139.
- (3) (a) van de Sande-Bruinsma, N.; Grundmann, H.; Verloof, D.; Tiemersma, E.; Monen, J.; Goossens, H.; Ferech, M. European Antimicrobial Resistance Surveillance System, G.; European Surveillance of Antimicrobial Consumption Project, G. Antimicrobial drug use and resistance in Europe. *Emerging Infect. Dis.* **2008**, *14*, 1722–1730. (b) Albrich, W. C.; Monnet, D. L.; Harbarth, S. Antibiotic selection pressure and resistance in *Streptococcus pneumoniae* and *Streptococcus pyogenes*. *Emerging Infect. Dis.* **2004**, *10*, 514–517. (c) Goossens, H.; Ferech, M.; Vander Stichele, R.; Elseviers, M. Outpatient antibiotic use in Europe and association with resistance: a cross-national database study. *Lancet* **2005**, *365*, 579–587.
- (4) Gatadi, S.; Gour, J.; Nanduri, S. Natural product derived promising anti-MRSA drug leads: A review. *Bioorg. Med. Chem.* **2019**, *27*, 3760–3774.
- (5) Centers for Disease Control and Prevention. *Staphylococcus aureus* resistant to vancomycin—United States, 2002. *MMWR Morb. Mortal. Wkly. Rep.* **2002**, *51*, S65–S67.
- (6) (a) Boucher, H. W.; Talbot, G. H.; Bradley, J. S.; Edwards, J. E.; Gilbert, D.; Rice, L. B.; Scheld, M.; Spellberg, B.; Bartlett, J. Bad bugs, no drugs: no ESKAPE! An update from the Infectious Diseases Society of America. *Clin. Infect. Dis.* **2009**, *48*, 1–12. (b) Zurenko, G. E.; Gibson, J. K.; Shinabarger, D. L.; Aristoff, P. A.; Ford, C. W.; Tarpley, W. G. Oxazolidinones: a new class of antibacterials. *Curr. Opin. Pharmacol.* **2001**, *1*, 470–476. (c) Zhao, Q.; Xin, L.; Liu, Y.; Liang, C.; Li, J.; Jian, Y.; Li, H.; Shi, Z.; Liu, H.; Cao, W. Current Landscape and Future Perspective of Oxazolidinone Scaffolds Containing Antibacterial Drugs. *J. Med. Chem.* **2021**, *64*, 10557–10580. (d) Gordeev, M. F.; Yuan, Z. Y. New Potent Antibacterial Oxazolidinone (MRX-1) with an Improved Class Safety Profile. *J. Med. Chem.* **2014**, *57*, 4487–4497.
- (7) Duval, R. E.; Grare, M.; Demore, B. Fight Against Antimicrobial Resistance: We Always Need New Antibacterials but for Right Bacteria. *Molecules* **2019**, *24*, 3152.
- (8) Egu, S. A.; Ibezim, A.; Onoabedje, E. A.; Okoro, U. C. Biological and *in silico* Evaluation of Quinolinedione and Naphthoquinone Derivatives as Potent Antibacterial Agents. *ChemistrySelect* **2017**, *2*, 9222–9226.
- (9) Borba-Santos, L. P.; Nicoletti, C. D.; Vila, T.; Ferreira, P. G.; Araújo-Lima, C. F.; Galvão, B. V. D.; Felzenszwalb, I.; de Souza, W.; de Carvalho da Silva, F.; Ferreira, V. F.; et al. A novel naphthoquinone derivative shows selective antifungal activity against Sporothrix yeasts and biofilms. *Braz. J. Microbiol.* **2022**, *53*, 749–758.
- (10) (a) Alfadhli, A.; Mack, A.; Harper, L.; Berk, S.; Ritchie, C.; Barklis, E. Analysis of quinolinequinone reactivity, cytotoxicity, and anti-HIV-1 properties. *Bioorg. Med. Chem.* **2016**, *24*, S618–S625. (b) Fröhlich, T.; Reiter, C.; Saeed, M. E. M.; Hutterer, C.; Hahn, F.; Leidenberger, M.; Friedrich, O.; Kappes, B.; Marschall, M.; Efferth, T.; Tsogoeva, S. B. Synthesis of Thymoquinone-Artemisinin Hybrids: New Potent Antileukemia, Antiviral, and Antimalarial Agents. *ACS Med. Chem. Lett.* **2018**, *9*, 534–539.
- (11) (a) Hoyt, M. T.; Palchadhuri, R.; Hergenrother, P. J. Cribrostatin 6 induces death in cancer cells through a reactive oxygen species (ROS)-mediated mechanism. *Invest. New Drugs* **2011**, *29*, 562–573. (b) Shrestha, J. P.; Subedi, Y. P.; Chen, L.; Chang, C.-W. T. A mode of action study of cationic anthraquinone analogs: a new class of highly potent anticancer agents. *MedChemComm* **2015**, *6*, 2012–2022.
- (12) (a) Santoso, K. T.; Menorca, A.; Cheung, C. Y.; Cook, G. M.; Stocker, B. L.; Timmer, M. S. M. The synthesis and evaluation of quinolinequinones as anti-mycobacterial agents. *Bioorg. Med. Chem.* **2019**, *27*, 3532–3545. (b) Valderrama, J. A.; Delgado, V.; Sepulveda, S.; Benites, J.; Theoduloz, C.; Buc Calderon, P.; Muccioli, G. G. Synthesis and Cytotoxic Activity on Human Cancer Cells of Novel Isoquinolinequinone-Amino Acid Derivatives. *Molecules* **2016**, *21*, 1199. (c) Ko, J. H.; Yeon, S. W.; Ryu, J. S.; Kim, T. Y.; Song, E. H.; You, H. J.; Park, R. E.; Ryu, C. K. Synthesis and biological evaluation of 5-arylamino-6-chloro-1H-indazole-4,7-diones as inhibitors of protein kinase B/Akt. *Bioorg. Med. Chem. Lett.* **2006**, *16*, 6001–6005. (d) de Almeida, P. D. O.; Dos Santos Barbosa Jobim, G.; Dos Santos Ferreira, C. C.; Rocha Bernardes, L.; Dias, R. B.; Schlaepfer Sales, C. B.; Valverde, L. F.; Rocha, C. A. G.; Soares, M. B. P.; Bezerra, D. P.; et al. A new synthetic antitumor naphthoquinone induces ROS-mediated apoptosis with activation of the JNK and p38 signaling pathways. *Chem.-Biol. Interact.* **2021**, *343*, 109444. (e) Novais, J. S.; Moreira, C. S.; Silva, A.; Loureiro, R. S.; Sa Figueiredo, A. M.; Ferreira, V. F.; Castro, H. C.; da Rocha, D. R. Antibacterial naphthoquinone derivatives targeting resistant strain Gram-negative bacteria in biofilms. *Microb. Pathog.* **2018**, *118*, 105–114.
- (13) Bayrak, N.; Ciftci, H. I.; Yildiz, M.; Yildirim, H.; Sever, B.; Tateishi, H.; Otsuka, M.; Fujita, M.; Tuyun, A. F. Structure based design, synthesis, and evaluation of anti-CML activity of the quinolinequinones as LY83583 analogs. *Chem.-Biol. Interact.* **2021**, *345*, No. 109555.
- (14) Mataraci-Kara, E.; Bayrak, N.; Yildirim, H.; Yildiz, M.; Ataman, M.; Ozbek-Celik, B.; Tuyun, A. F. Plastoquinone analogs: a potential antimicrobial lead structure intensely suppressing *Staphylococcus epidermidis* and *Candida albicans* growth. *Med. Chem. Res.* **2021**, *30*, 1728–1737.
- (15) (a) Jannuzzi, A. T.; Yildiz, M.; Bayrak, N.; Yildirim, H.; Shilkar, D.; Jayaprakash, V.; TuYuN, A. F. Anticancer agents based on Plastoquinone analogs with N-phenylpiperazine: Structure-activity relationship and mechanism of action in breast cancer cells. *Chem.-Biol. Interact.* **2021**, *349*, 109673. (b) Yildiz, M.; Bayrak, N.; Yildirim, H.; Mataraci-Kara, E.; Shilkar, D.; Jayaprakash, V.; Tuyun, A. F. Exploration of brominated Plastoquinone analogs: Discovery and structure-activity relationships of small antimicrobial lead molecules. *Bioorg. Chem.* **2021**, *116*, No. 105316.
- (16) (a) Bayrak, N.; Yildirim, H.; Tuyun, A. F.; Kara, E. M.; Celik, B. O.; Gupta, G. K.; Ciftci, H. I.; Fujita, M.; Otsuka, M.; Nasiri, H. R. Synthesis, Computational Study, and Evaluation of In Vitro Antimicrobial, Antibiofilm, and Anticancer Activities of New Sulfanyl Aminonaphthoquinone Derivatives. *Lett. Drug Des. Discovery* **2017**, *14*, 647–661. (b) Yildirim, H.; Bayrak, N.; Tuyun, A. F.; Kara, E. M.; Celik, B. O.; Gupta, G. K. 2,3-Disubstituted-1,4-naphthoquinones containing an arylamine with trifluoromethyl group: synthesis, biological evaluation, and computational study. *RSC Adv.* **2017**, *7*, 25753–25764. (c) Yildirim, H.; Yildiz, M.; Bayrak, N.; Mataraci-Kara, E.; Radwan, M. O.; Jannuzzi, A. T.; Otsuka, M.; Fujita, M.; TuYuN, A. F. Promising Antibacterial and Antifungal Agents Based on Thiolated Vitamin K3 Analogs: Synthesis, Bioevaluation, Molecular Docking. *Pharmaceuticals* **2022**, *15*, 586.
- (17) (a) Ciftci, H. I.; Bayrak, N.; Yildiz, M.; Yildirim, H.; Sever, B.; Tateishi, H.; Otsuka, M.; Fujita, M.; Tuyun, A. F. Design, synthesis and investigation of the mechanism of action underlying anti-leukemic effects of the quinolinequinones as LY83583 analogs. *Bioorg. Chem.* **2021**, *114*, 105160. (b) Mataraci-Kara, E.; Bayrak, N.; Yildiz, M.; Yildirim, H.; Ozbek-Celik, B.; Tuyun, A. F. Discovery and structure-activity relationships of the quinolinequinones: Promising antimicrobial agents and mode of action evaluation. *Drug Dev. Res.* **2022**, *83*, 628–636.

- (18) Yildirim, H.; Bayrak, N.; Yildiz, M.; Yilmaz, F. N.; Mataraci-Kara, E.; Shilkar, D.; Jayaprakash, V.; TuYuN, A. F. Highly Active Small Aminated Quinolinequinones against Drug-Resistant *Staphylococcus aureus* and *Candida albicans*. *Molecules* **2022**, *27*, 2923.
- (19) Yildirim, H.; Yildiz, M.; Bayrak, N.; Mataraci-Kara, E.; Ozbek-Celik, B.; Otsuka, M.; Fujita, M.; Radwan, M. O.; TuYuN, A. F. Natural-product-inspired design and synthesis of thiolated coenzyme Q analogs as promising agents against Gram-positive bacterial strains: insights into structure-activity relationship, activity profile, mode of action, and molecular docking. *RSC Adv.* **2022**, *12*, 20507–20518.
- (20) (a) Bayrak, N.; Yildiz, M.; Yildirim, H.; Kara, E. M.; Celik, B. O.; Tuyun, A. F. Brominated plastoquinone analogs: Synthesis, structural characterization, and biological evaluation. *J. Mol. Struct.* **2020**, *1219*, No. 128560. (b) Kara, E. M.; Bayrak, N.; Yildirim, H.; Yildiz, M.; Celik, B. O.; Tuyun, A. F. Chlorinated plastoquinone analogs that inhibit *Staphylococcus epidermidis* and *Candida albicans* growth. *Folia Microbiol.* **2020**, *65*, 785–795.
- (21) Bayrak, N.; Yildiz, M.; Yildirim, H.; Mataraci-Kara, E.; Tuyun, A. F. Novel plastoquinone analogs containing benzocaine and its analogs: structure-based design, synthesis, and structural characterization. *Res. Chem. Intermed.* **2021**, *47*, 2125–2141.
- (22) Cheng, Q.; Sandalova, T.; Lindqvist, Y.; Arner, E. S. Crystal structure and catalysis of the selenoprotein thioredoxin reductase 1. *J. Biol. Chem.* **2009**, *284*, 3998–4008.
- (23) Uziel, O.; Borovok, I.; Schreiber, R.; Cohen, G.; Aharonowitz, Y. Transcriptional regulation of the *Staphylococcus aureus* thioredoxin and thioredoxin reductase genes in response to oxygen and disulfide stress. *J. Bacteriol.* **2004**, *186*, 326–334.
- (24) Wang, X.; Wang, C.; Wu, M.; Tian, T.; Cheng, T.; Zhang, X.; Zang, J. Enolase binds to RnpA in competition with PNPase in *Staphylococcus aureus*. *FEBS Lett.* **2017**, *591*, 3523–3535.
- (25) Shaikh, I. A.; Johnson, F.; Grollman, A. P. Streptonigrin. 1. Structure-activity relationships among simple bicyclic analogues. Rate dependence of DNA degradation on quinone reduction potential. *J. Med. Chem.* **1986**, *29*, 1329–1340.
- (26) Kim, Y. S.; Park, S. Y.; Lee, H. J.; Suh, M. E.; Schollmeyer, D.; Lee, C. O. Synthesis and cytotoxicity of 6,11-dihydro-pyrido- and 6,11-dihydro-benzo[2,3-b]phenazine-6,11-dione derivatives. *Bioorg. Med. Chem.* **2003**, *11*, 1709–1714.
- (27) Yoon, E. Y.; Choi, H. Y.; Shin, K. J.; Yoo, K. H.; Chi, D. Y.; Kim, D. J. The regioselectivity in the reaction of 6,7-dihaloquinoline-5,8-diones with amine nucleophiles in various solvents. *Tetrahedron Lett.* **2000**, *41*, 7475–7480.
- (28) Lee, H. J.; Kim, J. S.; Park, S. Y.; Suh, M. E.; Kim, H. J.; Seo, E. K.; Lee, C. O. Synthesis and cytotoxicity evaluation of 6,11-dihydro-pyridazo- and 6,11-dihydro-pyrido[2,3-b]phenazine-6,11-diones. *Bioorg. Med. Chem.* **2004**, *12*, 1623–1628.
- (29) Kadela-Tomanek, M.; Jastrzębska, M.; Bębenek, E.; Chrobak, E.; Latocha, M.; Kusz, J.; Tarnawska, D.; Boryczka, S. New Acetylenic Amine Derivatives of 5,8-Quinolinediones: Synthesis, Crystal Structure and Antiproliferative Activity. *Crystals* **2017**, *7*, 15.
- (30) (a) Mataraci Kara, E.; Ozbek Celik, B. Investigation of the effects of various antibiotics against *Klebsiella pneumoniae* biofilms on *in vitro* catheter model. *J. Chemother.* **2018**, *30*, 82–88. (b) Costerton, J. W.; Lewandowski, Z.; Caldwell, D. E.; Korber, D. R.; Lappin-Scott, H. M. Microbial biofilms. *Annu. Rev. Microbiol.* **1995**, *49*, 711–745. (c) Donlan, R. M. Biofilms: microbial life on surfaces. *Emerging Infect. Dis.* **2002**, *8*, 881–890. (d) Sharma, D.; Misba, L.; Khan, A. U. Antibiotics versus biofilm: an emerging battleground in microbial communities. *Antimicrob. Resist. Infect. Control* **2019**, *8*, 76. (e) Pecoraro, C.; Carbone, D.; Deng, D.; Cascioferro, M. S.; Diana, P.; Giovannetti, E. Biofilm Formation as Valuable Target to Fight against Severe Chronic Infections. *Curr. Med. Chem.* **2022**, *29*, 4307–4310.
- (31) Bruker. APEX2, version 2014.1-1; Bruker AXS Inc.: Madison, WI, 2014.
- (32) Bruker. SAINT, version 8.34A; Bruker AXS Inc.: Madison, WI, 2013.
- (33) Bruker. SADABS, version 2012/2; Bruker AXS Inc.: Madison, WI, 2012.
- (34) Bruker. SHELXTL, version 6.14; Bruker AXS Inc.: Madison, WI, 2000.
- (35) Spek, A. L. Structure validation in chemical crystallography. *Acta Crystallogr., Sect. D: Biol. Crystallogr.* **2009**, *65*, 148–155.
- (36) Macrae, C. F.; Edgington, P. R.; McCabe, P.; Pidcock, E.; Shields, G. P.; Taylor, R.; Towler, M.; van de Streek, J. Mercury: visualization and analysis of crystal structures. *J. Appl. Crystallogr.* **2006**, *39*, 453–457.
- (37) Clinical and Laboratory Standards Institute (CLSI). *Performance Standards for Antimicrobial Susceptibility Testing*; Clinical and Laboratory Standards Institute: Wayne, PA, 2020.
- (38) Clinical and Laboratory Standards Institute (CLSI). *Reference Method for Broth Dilution Antifungal Susceptibility Testing of Yeasts; Approved Standard—Second Edition*; Clinical and Laboratory Standards Institute: Wayne, PA, 1997.
- (39) Kara, E. M.; Bayrak, N.; Yildirim, H.; Yildiz, M.; Celik, B. O.; Tuyun, A. F. Chlorinated plastoquinone analogs that inhibit *Staphylococcus epidermidis* and *Candida albicans* growth. *Folia Microbiol.* **2020**, *65*, 785–795.
- (40) Ropp, P. J.; Spiegel, J. O.; Walker, J. L.; Green, H.; Morales, G. A.; Milliken, K. A.; Ringe, J. J.; Durrant, J. D. Gypsum-DL: an open-source program for preparing small-molecule libraries for structure-based virtual screening. *J. Cheminf.* **2019**, *11*, 34.
- (41) Pettersen, E. F.; Goddard, T. D.; Huang, C. C.; Couch, G. S.; Greenblatt, D. M.; Meng, E. C.; Ferrin, T. E. UCSF Chimera—a visualization system for exploratory research and analysis. *J. Comput. Chem.* **2004**, *25*, 1605–1612.
- (42) Santos-Martins, D.; Solis-Vasquez, L.; Tillack, A. F.; Sanner, M. F.; Koch, A.; Forli, S. Accelerating AutoDock4 with GPUs and Gradient-Based Local Search. *J. Chem. Theory Comput.* **2021**, *17*, 1060–1073.
- (43) Salentin, S.; Schreiber, S.; Haupt, V. J.; Adasme, M. F.; Schroeder, M. PLIP: fully automated protein-ligand interaction profiler. *Nucleic Acids Res.* **2015**, *43*, W443–W447.